# **DNA Damage-induced Expression of p53 Suppresses Mitotic Checkpoint Kinase hMps1**

THE LACK OF THIS SUPPRESSION IN \$53^MUT CELLS CONTRIBUTES TO APOPTOSIS\*S

Received for publication, October 18, 2005, and in revised form, January 4, 2006 Published, JBC Papers in Press, January 30, 2006, DOI 10.1074/jbc.M511333200

Mandar R. Bhonde<sup>‡</sup>, Marie-Luise Hanski<sup>‡</sup>, Jan Budczies<sup>§</sup>, Minh Cao<sup>‡</sup>, Bernd Gillissen<sup>¶</sup>, Dhatchana Moorthy<sup>‡</sup>, Federico Simonetta<sup>||</sup>, Hans Scherübl<sup>‡</sup>, Matthias Truss\*\*, Christian Hagemeier\*\*, Hans-Werner Mewes<sup>s</sup>, Peter T. Daniel, Martin Zeitz, and Christoph Hanski

From the <sup>‡</sup>Department of Gastroenterology, University Medical Center Charité, Campus Benjamin Franklin, 12200 Berlin, Germany,  $^{\S}$ Institute for Bioinformatics, GSF-National Research Center for Environment and Health, 85764 Neuherberg, Germany,  $^{\P}$ University Medical Center Charité, Campus Virchow Klinikum, 13353 Berlin, Germany, <sup>II</sup>Department of Internal Medicine, Division of Internal Medicine and Clinical Immunology, University of Genoa, 16132 Genoa, Italy, and \*\*Children's Hospital, Laboratory for Molecular Biology, Charité-CCM, Humboldt University, 10117 Berlin, Germany

DNA damage induced by the topoisomerase I inhibitor irinotecan (CPT-11) triggers in p53 WT colorectal carcinoma cells a long term cell cycle arrest and in p53<sup>MUT</sup> cells a transient arrest followed by apoptosis (Magrini, R., Bhonde, M. R., Hanski, M. L., Notter, M., Scherübl, H., Boland, C. R., Zeitz, M., and Hanski, C. (2002) Int. J. Cancer 101, 23-31; Bhonde, M. R., Hanski, M. L., Notter, M., Gillissen, B. F., Daniel, P. T., Zeitz, M., and Hanski, C. (2006) Oncogene 25, 165-175). The mechanism of the p53-independent apoptosis still remains largely unclear. Here we used five p53WT and five p53MUT established colon carcinoma cell lines to identify gene expression alterations associated with apoptosis in p53<sup>MUT</sup> cells after treatment with SN-38, the irinotecan metabolite. After treatment, 16 mitosis-related genes were found to be expressed at least 2-fold stronger in the apoptosis-executing p53<sup>MUT</sup> cells than in the cell cycle-arrested  $p53^{\mathrm{WT}}$  cells by oligonucleotide microarray analysis. One of the genes whose strong post-treatment expression was associated with apoptosis was the mitotic checkpoint kinase hMps1 (human ortholog of the yeast monopolar spindle 1 kinase). hMps1 mRNA and protein expression were suppressed by the treatment-induced and by the exogenous adenovirus-coded p53 protein. The direct suppression of hMps1 on RNA level or inhibition of its activity by a dominant-negative hMps1 partly suppressed apoptosis. Together, these data indicate that the high expression of mitotic genes in p53<sup>MUT</sup> cells after SN-38 treatment contributes to DNA damageinduced apoptosis, whereas their suppression in p53WT cells acts as a safeguard mechanism preventing mitosis initiation and the subsequent apoptosis. hMps1 kinase is one of the mitotic checkpoint proteins whose expression after DNA damage in p53 MUT cells activates the checkpoint and contributes to apoptosis.

The function of p53 protein as a guardian of the genome is to prevent the organism from propagation of potentially harmful DNA lesions. The p53WT 2 cells react to a mutagenic offense by a cell cycle arrest,

allowing for the proper repair of the damaged DNA, or in the case of overwhelming damage by apoptosis triggered by the p53-mediated activation of proapoptotic genes such as BAX, PUMA, and NOXA (3).

The majority of colorectal carcinomas have a mutated p53 gene that in most of the cases is associated with a loss of tumor suppressor function. These cells are unable to execute a proper cell cycle arrest after DNA damage and are also frequently resistant to apoptosis, which results in propagation of genetic lesions and cell survival.

We showed previously that despite this general concept, colon carcinoma cells may respond differently to the chemotherapeutic irinotecan (CPT-11); the p53<sup>WT</sup> cells execute a long term cell cycle arrest after irinotecan treatment, whereas the p53-deficient cells perform a transient cell cycle arrest followed by apoptosis (1).

Because of the frequent p53 mutations in colon carcinoma cells, the p53-independent apoptosis is of particular interest. The p53 $^{
m MUT}$ cells usually do not maintain the G<sub>2</sub>/M arrest after DNA damage, but initiate a premature mitosis that leads to mitotic catastrophe, accompanied by the emergence of aberrant mitoses and distinct nuclear forms of micronucleation and apoptotic nuclear condensa-

Mitotic catastrophe can be also induced in p53<sup>WT</sup> cells by DNA damage and is concomitant with elimination of genes responsible for triggering of  $G_2/M$  arrest, like Chk1 or ATR (7, 8), or those responsible for its maintenance, like p21 $^{\mathrm{WAF1/Cip1}}$  (9) or 14-3-3 $\sigma$  (10), or by a direct interference with mitosis regulation through depletion of genes like survivin (11), MAD2 (12), polo-like kinase-1 (13), or polo-like kinase-2 (14).

The details of the relationship between mitotic catastrophe and apoptosis pathways are not elucidated. In some systems, DNA damageinduced mitotic catastrophe and apoptosis can be uncoupled; apoptosis could be inhibited at the Bcl-2 level (15) or at the caspase 9 level (16) without inhibition of mitotic cell death. Thus, the mitotic catastrophe may trigger a cell death signaling pathway not identical with that of the classical apoptosis. On the other hand, the similarity of nuclear morphologies and common biochemical markers of the consecutive steps of classical apoptosis and of mitotic catastrophe-associated cell death indicate that they share common signaling steps (6).

In order to identify genes associated with DNA damage-induced apoptosis of p53<sup>MUT</sup> cells, we compared the transcriptional response profiles of five p53WT colorectal carcinoma cell lines, which after damage

interfering RNA; RT, reverse transcriptase; m.o.i., multiplicity of infection; GFP, green fluorescent protein; DAPI, 4,6-diamidino-2-phenylindole; PARP, poly(ADP-ribose) polymerase; PBS, phosphate-buffered saline; DMEM, Dulbecco's modified Eagle's medium; FCS, fetal calf serum.



<sup>\*</sup> This work was supported by the NGFN1 Program of the Bundesministerium für Bildung und Forschung and the Sonnenfeld Stiftung and the Monika Kutzner Stiftung. The costs of publication of this article were defrayed in part by the payment of page charges. This article must therefore be hereby marked "advertisement" in accordance with 18 U.S.C. Section 1734 solely to indicate this fact.

The online version of this article (available at http://www.jbc.org) contains Tables S1 and S2 and Figs. S1–S5.

<sup>&</sup>lt;sup>1</sup> To whom correspondence should be addressed: Charité-Universitaetsmedizin Berlin, Campus Benjamin Franklin, Dept. of Gastroenterology, Hindenburgdamm 30, 12200 Berlin, Germany. Tel.: 49-30-8445-4522; Fax: 49-30-8445-4582; E-mail: christoph.

<sup>&</sup>lt;sup>2</sup> The abbreviations used are: p53<sup>WT</sup>, wild-type p53; p53<sup>MUT</sup>, mutated p53; siRNA, small

underwent long term arrest, and five p53-defective cell lines, which responded to treatment with apoptosis.

The regulation and the role of the mitotic checkpoint kinase hMps1 in DNA damage-induced mitotic catastrophe/apoptosis were addressed in detail. hMps1 kinase, also called PYT or TTK, is one of the molecules controlling the mitotic checkpoint. Upon its activation, hMps1 is recruited from the cytosol to the kinetochores (17) and in the metaphase also to centrosomes (18). It interacts there with other kinetochore proteins CENP-E, BubR1, Bub1p, and Bub3p (19) and additionally recruits Mad1 and Mad2 to kinetochores (17). The suppression of hMps1 in the presence of the mitotic checkpoint activator nocodazole leads to a premature mitotic exit followed by micronucleation (20).

Here, for the first time, we have identified hMps1 as one of the genes negatively regulated by the p53 protein after DNA damage by SN-38. Moreover, we show that the lack of suppression of hMps1 in p53-deficient cells contributes to damage-induced apoptosis.

#### **EXPERIMENTAL PROCEDURES**

Cell Lines, p53 Status, and Culture Conditions—The following p53WT cell lines and growth conditions were used: HCT116 (DMEM + 10% FCS), LS174T (DMEM + 10% FCS), SW48 (Leibovitz L15 + 10% FCS), Co115 (DMEM + 10% FCS), HCT8 (RPMI + 10% FCS), and HCT116p21<sup>-/-</sup> (McCoy 5A + 10% FCS + 400  $\mu$ g/ml G418 + 100  $\mu$ g/ml hygromycin B). The p53-deficient cell lines were HCT116p53<sup>-/-</sup> (DMEM + 10% FCS +  $400 \,\mu \text{g/ml} \,\text{G}418 + 100 \,\mu \text{g/ml} \,\text{hygromycin B}$ , HT-29 (RPMI + 10% FCS), WiDr (minimum Eagle's medium + 10% FCS + nonessential amino acids), SW480 (DMEM + 10% FCS), HCT15 (RPMI + 20% FCS), and HeLa (DMEM + 10% FCS). All cell lines were cultivated in 5% CO<sub>2</sub>, except the SW48 cell line, which was kept in the normal atmosphere.

Chemicals and Treatment of Cultured Cells—One day after seeding, the cells were treated for 2 days with 10 nm SN-38, washed with PBS, and then incubated in drug-free media for the indicated time points. For certain experiments, cells were continuously treated with 10 nm SN-38 for the required time period.

Flow Cytometry—For cell cycle analysis, adherent cells were trypsinized and pooled with the floating cells. Cell suspension of  $1 \times 10^6$  cells was washed with PBS, fixed in ice-cold 70% ethanol at -20 °C, and stained with a 20  $\mu$ g/ml propidium iodide, 0.1% Triton X-100, 200  $\mu$ g/ml RNase A solution. Stained cells were analyzed using a FACScan (BD Biosciences) and the ModFit LT2 software (Verity Software House, Topsham, ME) as described recently (2). For staining of phosphorylated histone H3, only adherent cells were trypsinized and fixed in 70% ethanol, washed in PBS, and treated for 10 min with 0.25% Triton X-100. After washing with 1% bovine serum albumin in PBS, the cells were incubated for 1 h with antibody against phosphorylated histone H3 (Ser-10) (Santa Cruz Biotechnology, Heidelberg, Germany), followed by a 30-min incubation with fluorescein isothiocyanate-conjugated anti-rabbit IgG (Dianova, Hamburg, Germany). The cells were then stained with propidium iodide for 30 min as mentioned above and analyzed.

Western Blotting-For analysis of total lysates, adherent cells were scraped off and pooled with the floating cells and lysed in lysis buffer described previously (21) for 15 min on ice. Lysates were precleared by centrifugation at 13,000  $\times$  g for 30 min at 4 °C. Proteins were separated on SDS-polyacrylamide gels and electroblotted onto Immobilon-P membrane (Millipore, Eschborn, Germany), which was blocked with 5% nonfat dry milk in 0.1% Tween 20 in TBS for 1 h, followed by overnight incubation at 4 °C with the corresponding first antibody. The antibodies used were as follows: mouse monoclonal anti-PARP (BD Biosciences), mouse monoclonal anti-hMps1 antibody (NT, clone 3-472-1; Upstate Cell Signaling Solutions, Waltham, MA), and anti-p16 antibody and

anti-BubR1-antibody (BD Biosciences). Other antibodies used here, the signal detection, densitometric analysis, and the evaluation of PARP fragmentation were described recently (2, 22).

Oligonucleotide Microarrays Target Preparation—Total RNA was isolated from nontreated and SN-38-treated cells by using RNA Clean LS reagent (Hybaid, Heidelberg, Germany). The floating, already apoptotic cells were discarded because they contained degraded RNA (data not shown). Double-stranded cDNA was synthesized from 10 µg of total RNA (Superscript Choice System, Invitrogen), followed by the synthesis of biotin-labeled cRNA in an in vitro transcription reaction (ENZO BioArray HighYield RNA transcript labeling kit, Affymetrix, Santa Clara, CA). The cRNA targets were purified using RNeasy columns (Qiagen, Hilden, Germany) and fragmented by heating at 94 °C for 35 min. The targets were hybridized to GeneChip HU95Av2 oligonucleotide microarrays in the Gene Fluidics Station 400 (GeneChip Instrument System, Affymetrix, Santa Clara).

Analysis of the GeneChip Data—Image intensities of the hybridization patterns obtained by laser scanning (HP GeneArray scanner, Affymetrix) were stored in raw data files.

Preprocessing and analysis of the expression data were performed using the statistical language R (www.R-project.org (23)). The signals were substituted by a single expression value termed robust multiarray average (24, 25). The robust multiarray average values, which were background-adjusted, normalized, and log-transformed summary measures for the perfect match hybridization, were used as input for further processing and analysis. Hybridization values of all cell lines were normalized to the values of HCT116 p53<sup>-/-</sup> cells before treatment as described (26).

To detect significant differences in gene expression after treatment between the two groups, a combined ratio of expression and p value threshold was used. The ratio of expression was defined as mean of the robust multiarray average expression values in five p53<sup>MUT</sup> cell lines, exponentiated back to the linear scale and divided by the mean of the corresponding values in five  $p53^{WT}$  cell lines. The p values were obtained by the Welch's two-sample t test. Expression ratios and p values were calculated separately for both the SN-38-treated and nontreated cell lines.

The results of the selection procedures were first validated by a permutation analysis. The number of selected genes in each of 126 informative permutations of cell lines was calculated. Then, the observed number  $(n_{obs})$ of genes expressed differentially between p53<sup>WT</sup> and p53<sup>MUT</sup> cell lines was compared with the mean number expected ( $n_{\mathrm{exp}}$ ) from the permutation at null distribution. A p value was calculated to assess the significance of finding  $n_{\rm obs}$  or more differentially expressed genes. The false discovery rate of the selection procedure was estimated by the quotient  $n_{\rm obs}/n_{\rm exp}$ .

An agglomerative hierarchical clustering of probe sets and cell lines was performed by the algorithm hclust implemented in R (27). The clustered gene profiles were visualized in a red-green plot, with the mean value of each gene expression in all cell lines encoded in black, expression above in red, and expression below in green.

Validation of Microarray Data by RT-PCR—The correctness of gene expression data obtained was tested by semi-quantitative RT-PCR from the same RNA that was used for cRNA target preparation. The list of validated genes is shown in supplemental Table S1.

Real Time PCR-Analysis of gene expression on mRNA levels was done by performing real time one-step RT-PCR (QuantiTect SYBR Green RT-PCR kit, Qiagen, Hilden, Germany). Briefly, 50 ng of total RNA was reverse-transcribed using gene-specific primers, followed by amplification for 40 cycles in a real time cycler (Mastercycler ep realplex, Eppendorf, Germany). The amounts of mRNA after treatment relative to those prior to treatment were calculated as  $R = 2^{-\Delta \Delta Ct}$  (i.e. ) for each sample.



Overexpression of p53 and p21WAF1/Cip1 Proteins Using Adenovirus Expression System-HCT116, HCT116p53-/-, and HCT-116 p21<sup>WAF1/Cip1-/-</sup> cells were infected with Ad-p53<sup>WT</sup> or Ad-p21<sup>WAF1/Cip1WT</sup> as described (28). Cells were seeded, and after 24 h they were incubated with the adenovirus (AdCMVp21WAF1/Cip1, AdCMVp53, or AdLacZ as a control) at the desired multiplicity of infection (m.o.i.) for 90 min at 37 °C in medium without serum. The cells were harvested for preparation of lysates or for isolation of total RNA 2 days after infection.

Nuclear Staining—Cytospins prepared on glass slides or cells grown in dishes were fixed in ice-cold methanol for 20 min, washed three times in PBS, stained with 0.5  $\mu$ g/ml DAPI in PBS for 15 min, washed again, and mounted. At least 200 nuclei were microscopically evaluated by at least two observers (Olympus BX60F5; Optical Co. GmbH, Hamburg, Germany). Photographs were taken by using analySIS® image processing software (Soft Imaging Systems, Münster, Germany).

Immunofluorescence Staining-Adherent cells were fixed with 4% formaldehyde, 1 mm MgCl<sub>2</sub>, and 0.5% Triton X-100 in PBS for 10 min. Cytospins were fixed in ice-cold methanol for 6 min (for anti-PARP fragment p89 staining) or in 4% formaldehyde, 1 mM MgCl<sub>2</sub>, and 0.5% Triton X-100 solution (for anti-centromere and anti-BubR1 staining) followed by permeabilization in 0.5% Triton X-100 for 10 min. Cells were washed with PBS and incubated in blocking solution (5% donkey serum + 0.1% Triton X-100 in TBS) or 5% donkey serum in TBS, 0.1% Tween 20) for 20 min. Antibodies used for immunofluorescence were rabbit anti-PARP-p89 fragment (Promega, Mannheim, Germany), mouse monoclonal anti-BubR1 (BD Biosciences), and human anti-centromere antiserum (Antibodies Inc., Seattle). The cells were incubated with the first antibody in blocking solution for 1 h, followed by the second antibody (donkey anti-mouse-Cy3 or a biotin-conjugated antibody) for 45 min. The cells were then incubated with streptavidin-Cy3 or streptavidin-Alexa-488 for 20 min and then with DAPI (0.5  $\mu$ g/ml) for 15 min, mounted, and photographed under the microscope. All secondary antibodies and conjugates were purchased from Dianova, Hamburg, Germany.

Gene Suppression Using pSUPER Plasmid—Cells were transfected with 20 µg of pSUPER-hMps1 by electroporation. For electroporation, the cells were resuspended in serum-free RPMI at a density of  $3 \times 10^6$  cells/ml. Electroporation was carried out in a GenePulser II module (Bio-Rad) in the presence of the appropriate plasmid with  $1.2 \times 10^6$  cells at 290 V and 1050 microfarad capacitance. Then the cells were transferred to 35-mm dishes containing appropriate prewarmed complete medium and incubated at 37 °C, 5% CO<sub>2</sub> for 24 h. Cells were washed and cultured in medium containing SN-38 and were harvested 2 and 3 days after treatment. Electroporation yields a transfection efficiency with pSUPER plasmids of 70% (data not shown). To control the off-target effects of transfection, cells were transfected under identical conditions with pSUPER-EGFP plasmid or pSUPER-hMLH1 plasmid and pSUPER-mCMV56 plasmid.

Caspase Activity Assay—The extent of apoptosis was determined by assaying caspase 3 and caspase 7 activities using FLICA apoptosis detection kit (Immunochemistry Technologies, Bloomington, MN), based on staining of cells with a substrate for detection of caspase 3 and 7 as recommended, and the green fluorescence was measured in a FACScan.

Recovery of Mitotic Cells—Following treatment with nocodazole (333 nm; 16 h) or SN-38 (10 nm; 48 h), the cell culture flasks were mechanically agitated for 15 min. The cells released into the culture medium were recovered and lysed. Cytospins of an aliquot of the mitotic cells stained with DAPI showed that 60-80% of the cells were in mitosis (data not shown).

Inhibition of Endogenous hMps1 Activity by Overexpression of hMps1-KD-24 h after seeding, HCT116p53-/- cells were transfected either with pcDNA-GFP (a kind gift from Dr. Marian Martinez-Balbas, Institute of Molecular Biology, Barcelona, Spain) or with pcDNA-hMps1 (Myc-tagged WT hMps1) or pcDNA-hMps1-KD (Myc-tagged dominantnegative kinase-dead mutant of the hMps1 protein; both were a kind gift from Dr. E. Nigg, Max Planck Institute for Biochemistry, Martinsried, Germany) by electroporation as mentioned above. 24 h after transfection, the cells were treated with 10 nm SN-38 for 2 and 3 days. Cytospins were made and stained with anti-Myc antibody (Invitrogen) to detect the hMps1-KDtransfected cells. Nuclei were stained with DAPI. The nuclear morphologies of the GFP-transfected cells and the hMps1-KD-transfected cells were compared by microscopy as mentioned above. To offset variable transfection efficiency, only the transfected cells were investigated after staining with the anti-Myc antibody, which detected only exogenously expressed proteins (hMps1 or hMps1-KD).

#### **RESULTS**

Cellular Reaction of Colon Carcinoma Cell Lines to Treatment with SN-38 Is Affected by the p53 Function—Previous data obtained with two p53<sup>WT</sup> cell lines (HCT116 and LS174T) and two p53-deficient cell lines (HCT116p53<sup>-/-</sup> and HT-29) showed that DNA damage induced by topoisomerase I inhibitor irinotecan (CPT-11) or its active metabolite SN-38 leads to a long term cell cycle arrest in the p53 WT cells or short term arrest followed by apoptosis in the p53<sup>MUT</sup> cells (1, 2).

To analyze how general this observation is, three additional p53WT and three p53<sup>MUT</sup> colon carcinoma cell lines were selected, and their response was analyzed after treatment with SN-38. As described previously for the four cell lines (2), in the additional six cell lines, SN-38 also induced a p53-independent G<sub>2</sub>/M arrest within 2 days (see Ref. 2 and data not shown) after start of treatment (Fig. 1, A and B, and supplemental Fig. S1). After 4 days, however, in the  $p53^{\mathrm{WT}}$  cell lines the markers of G<sub>2</sub>/M arrest (CDK1 and cyclin B1) were suppressed, whereas the markers of  $G_1$  arrest (cyclin D1 and p27) were overexpressed (Fig. 2), i.e. a transient  $G_2/M$  arrest was followed by arrest in a tetraploid  $G_1$  phase. This arrest lasted for several days (data not shown). Interestingly, the p16 protein was absent in these cell lines, except at very low level in LS174T, indicating that the long term arrest was p16-independent.

By contrast, in all p53<sup>MUT</sup> cell lines a consistent up-regulation of the cyclin B1, CDK1, and histone H3 phosphorylation and down-regulation of p27 protein and cyclin D1 were evident 4 days after start of treatment (Fig. 2 and supplemental Fig. S2), indicating that the surviving cells were in the G<sub>2</sub>/M phase of the cell cycle. Concomitantly, extensive PARP cleavage, which is a hallmark of apoptosis, was detectable (Fig. 1F), i.e. the G<sub>2</sub>/Marrested cells proceeded to mitosis and to apoptosis (see below).

These two groups of cell lines with a defined p53 status and the characteristic behavior after SN-38 treatment were used as a model system. We used it to define a common transcriptional profile of each cell group after treatment.

Apoptosis in p53-deficient Cells Is Accompanied by the Appearance of Distinct Nuclear Morphologies—We characterized the change of nuclear morphology of the p53-defective cells after SN-38 treatment. Four types of nuclear forms could be clearly discerned as follows: tetraploid interphase nuclei (Fig. 3, B versus A), aberrant mitoses (Fig. 3C), micronucleated cells, and nuclei with condensed chromatin (Fig. 3D). Of these morphological forms, only cells with condensed nuclei showed evidence for apoptosis, demonstrated through in situ detection of the cleaved 89-kDa PARP fragment (Fig. 3, D and E). The time course of the emergence of the nuclear forms after treatment showed that the percentage of micronucleated cells and condensed nuclei continuously increased at the expense of other forms



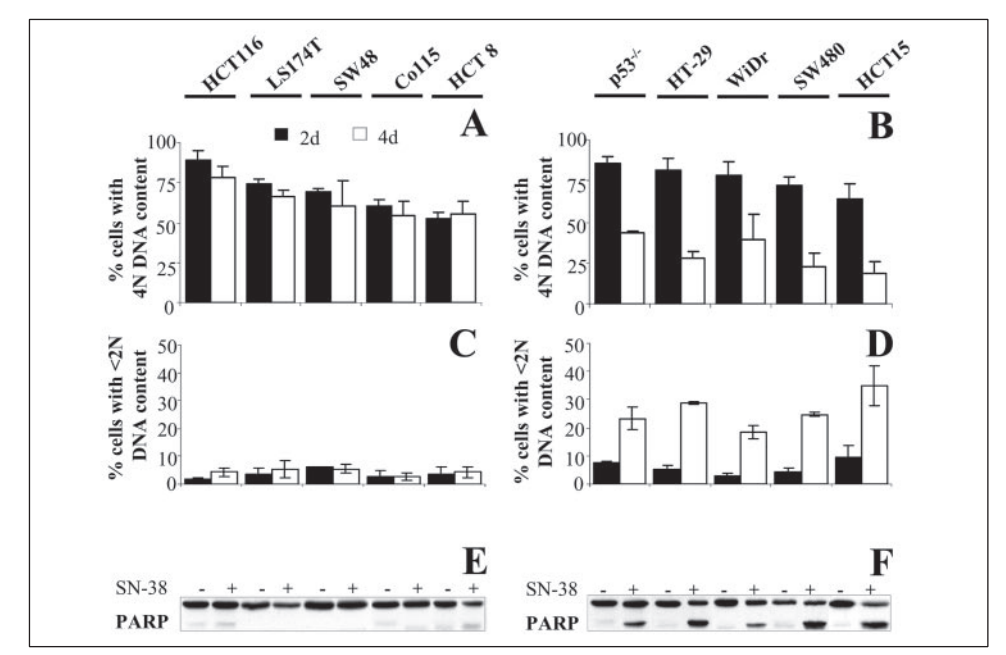


FIGURE 1. SN-38 treatment induces long term arrest or apoptosis in colon carcinoma cell lines. The tetraploid cell cycle arrest is maintained between 2 and 4 days after start of treatment in cell lines with intact p53 (A) but not in cells with defective or absent p53 (B). Only the p53-defective cells execute apoptosis as seen by the percentage of cells with DNA  $\leq 2N$  (C and D) and by detection of PARP cleavage (E and F). Results of three experiments  $\pm$  S.D. Western blots are representative of 2-3 experiments.

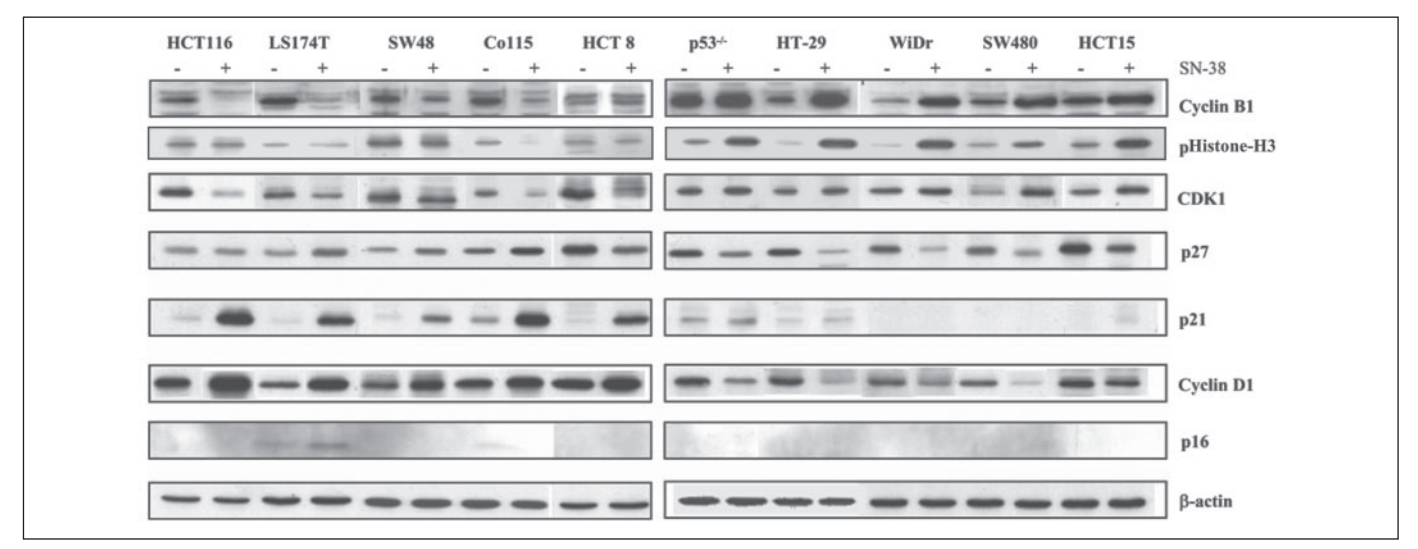


FIGURE 2. Expression of the cell cycle markers in the lysates of the viable, adherent cells indicates a tetraploid G<sub>1</sub> arrest in the p53<sup>WT</sup> (left panel) and a G<sub>2</sub>/M arrest in the p53<sup>MUT</sup> cell group (right panel) 4 days after start of treatment.

(Fig. 3F). The percentage of condensed nuclei was used in further experiments as an additional measure of the extent of apoptosis. These data indicated that in the investigated p53-deficient cell lines apoptosis is the end point of SN-38-induced DNA damage response.

Mitotic Checkpoint Is Activated after SN-38 Treatment—Aberrant mitoses preceded the condensed, apoptotic nuclei. We examined whether they emerged as a result of the activation of the mitotic checkpoint. All the investigated p53-deficient cell lines had a functional mitotic checkpoint; nocodazole, a known mitotic checkpoint activator induced mitotic arrest in all cell lines (supplemental Table S2). SN-38 treatment led to mitotic arrest in 5% of HCT116p53 $^{-/-}$  cells (Fig. 3F) and in 20% of HT-29 cells (not shown) or HeLa cells (see below). To test the function of the mitotic checkpoint, these mitoses were shaken off, and the cell population containing 60-80% mitoses was analyzed by Western blot and immunocytochemistry. Both the phosphorylation of BubR1 protein and its localization to the kinetochores indicated that in the cells released from the arrest into mitosis the mitotic checkpoint was activated (Fig. 4). Similar results were obtained with all other cell lines of

the p53-deficient group, except HCT-15 cells, in which the shake-off led to a high contamination of the mitotic population with the nonmitotic adherent cells (data not shown).

Different Gene Expression Profiles in p53-intact and p53-defective Cell Lines after SN-38 Treatment—We hypothesized that the dramatically different behavior of both cell groups is reflected by different gene expression after treatment. To analyze the treatment-related transcriptional response profiles, RNA was isolated prior to or 4 days after the start of treatment and processed for hybridization to oligonucleotide microarrays. At day 4,  $\mathrm{p53}^{\mathrm{WT}}$  cells are arrested in the tetraploid  $\mathrm{G}_{\mathrm{1}}$  phase, whereas the  $\mathrm{p53}^{\mathrm{MUT}}$ cells undergo apoptosis (Figs. 1 and 2 and supplemental Figs. S1 and S2). The target cRNAs were probed with the HU95Av2 chip, scanned, and statistically evaluated. We searched for genes with a ratio of expression in p53<sup>MUT</sup>/p53<sup>WT</sup>  $\geq$ 2 or  $\leq$ 0.5 and a significant difference in expression (p <0.01) between the two groups of treated cells. Seventy probe sets, corresponding to 64 genes, were identified (Table 1).

Statistical significance of the result was inferred from the permutation analysis (see "Experimental Procedures"). The number of selected genes



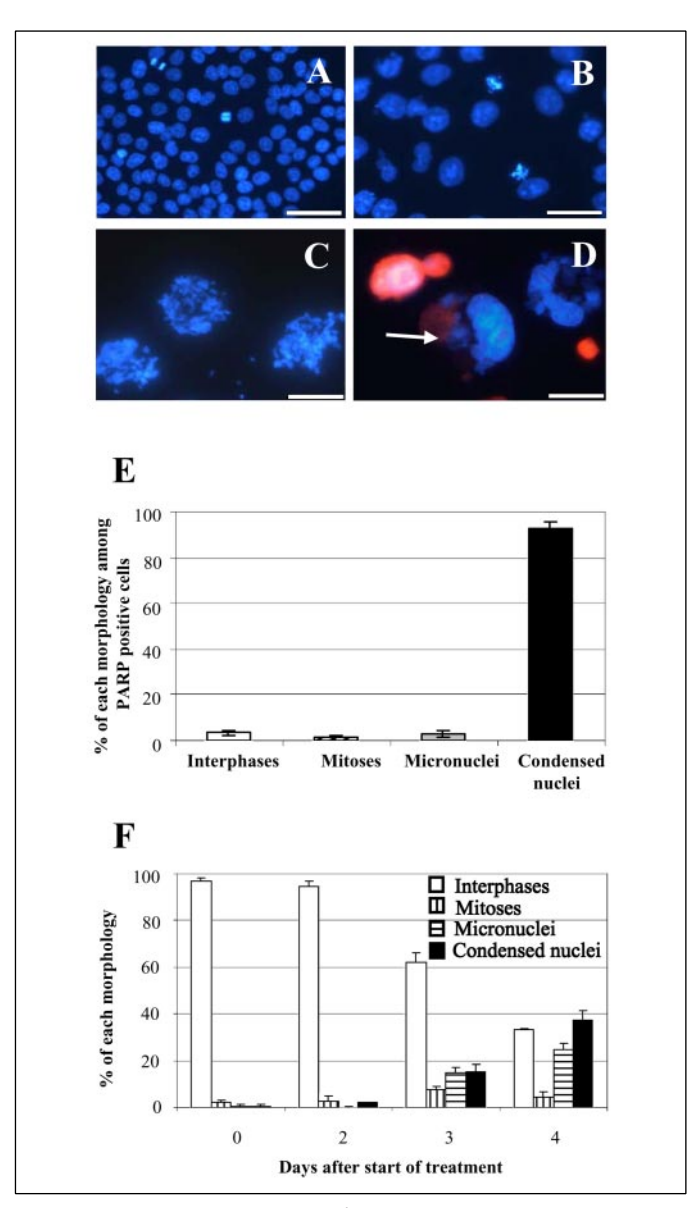


FIGURE 3. The treatment of HCT116p53<sup>-/-</sup> cells with SN-38 leads to the emergence of four morphological forms. A, nontreated; B, tetraploid cells 2 days after start of treatment, note the large size of the nuclei; C, aberrant mitoses, 2 days after start of treatment: D, micronucleated cells (arrow) and nuclei with condensed chromatin (red. stained for PARP fragment p89) 4 days after start of treatment; E, in nearly 100% of the nuclei with condensed chromatin the 89-kDa fragment of PARP was detectable; F, the time course indicates that the percentage of micronucleated cells and cells with condensed chromatin increases with time at the expense of other forms. Bar, 50  $\mu$ m (A and B) and 20  $\mu$ m (C and D).

turned out to be significantly higher than expected from the null distribution (p = 0.008), and the false discovery rate was estimated as 9%.

Interestingly, if the combined thresholds (ratio of expression  $\geq 2$ , p <0.01) were applied to the expression data before treatment, only five potentially differentially expressed genes were identified, which does not significantly exceed the number of genes identified in generically permutated data (p = 0.373) (data not shown). Thus, the specificity of the used algorithm was entirely due to the reaction of the cells to treatment and not to the basal differences in expression.

When the information on the ratio of gene expression before treatment was included as a second dimension, the scatter plot separated the selected genes into two groups: those in which the ratio of expression in p53<sup>MUT</sup>/ p53WT was smaller (supplemental Fig. S3A, squares) and those in which it was greater (triangles) after treatment than prior to treatment.

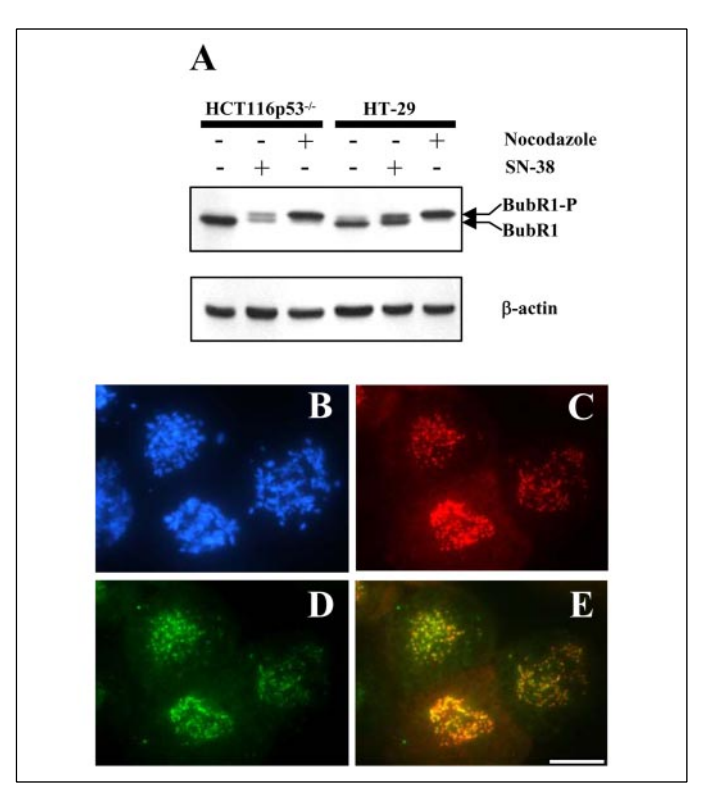


FIGURE 4. Cells slipping from the SN-38-induced G<sub>2</sub> arrest into mitosis have an activated mitotic checkpoint. A, BubR1 is phosphorylated in HCT116p53<sup>-/-</sup> HT-29 cells after 16 h of treatment with 333 nm nocodazole as well as after 48 h of SN-38 treatment. In both cases cell populations containing about 60-80% mitoses were analyzed after the shake off of the mitoses. Data are representative of two experiments. B. DAPI staining of the SN-38 treated cells: C. BubR1 staining: D. kinetochore staining. E. C. and D are merged to show the BUBR1 localization on kinetochores. Bar, 20  $\mu$ m.

Of the 64 genes in Table 1, 16 up-regulated genes were known to be directly or indirectly involved in different steps of mitosis (boldface type). This suggested that these mitosis-controlling genes are negatively regulated by p53 in response to DNA damage. Most of the genes from Table 1, which were more strongly expressed in the basal, nontreated state in p53<sup>MUT</sup> than in p53<sup>WT</sup> cells (i.e. which were possibly suppressed by the basal level of p53), were even more strongly overexpressed after treatment and showed a strong suppression in the p53 WT cells (supplemental Fig. S3A, red triangles). These are candidates for target genes negatively regulated by p53 after SN-38 treatment. This interpretation of the scatter plot was supported by a hierarchical clustering of the probes listed in Table 1 and the 10 cell lines (supplemental Fig. S3B). It shows that most of the genes up-regulated after treatment in one group of cell lines were down-regulated in the other group and vice versa.

Validation of the Selected Alterations on RNA and Protein Level-The validation of the array results was carried out in a semiquantitative RT-PCR on 34 genes, whose change of expression varied between 1.2- and 11.7-fold. (List of genes tested, the primers, and PCR conditions used are given in the supplemental Table S1.) Of the 122 tests performed, 111 confirmed the changes observed in the arrays, thus indicating that the correctness of the array results was 90% (data no shown). The expression of the mitotic checkpoint kinase hMps1, which was consistently suppressed in  $p53^{\rm WT}$  and overexpressed in  $p53^{\rm MUT}$  cells, was investigated in detail.

hMps1 mRNA and protein was up-regulated at 4 days after the start of treatment in all p53<sup>MUT</sup> cell lines and down-regulated in all p53<sup>WT</sup> cell lines (Fig. 5). This dichotomous behavior suggested that these alterations may be dependent on the p53 mutation status. Additionally, we hypothesized that it may be causally related to the different biological behavior of the two groups of cell lines.



**TABLE 1** Genes whose ratio of expression in p53 $^{MUT}$ /p53 $^{WT}$  after treatment is  $\geq$ 2 or  $\leq$ 0.5 and whose expression differs significantly between the two groups (p < 0.01) Genes involved in  $G_2/M$  arrest or in different steps of mitosis are printed in boldface.

No.	Affymetrix Probe ID	Gene symbol	Gene name		Ratio of
					expression after treatment
	39230_at	APOBEC3B	apolipoprotein B mRNA editing enzyme, catalytic polypeptide-like 3B	0.00509	5.5
	32263_at	Cyclin B2	cyclin B2	0.00057	5.48
	34736_at	Cyclin B1	cyclin B1	0.00711	4.72
	34852_g_at	AURORA	serine/threonine kinase 6	0.00007	4.59
	33845_at 40041_at	HNRPH1	heterogeneous nuclear ribonucleoprotein H1 (H) kinetochore associated 2 (Hec1)	0.00652 0.00026	4.41 4.31
	675 at	Hec1 IFITM1	interferon induced transmembrane protein 1 (9-27)	0.00026	4.31
	35699 at	BUB1B	BUB1 budding uninhibited by benzimidazoles 1 homolog beta (yeast)	0.00233	4.11
	40412 at	PTTG1	pituitary tumor-transforming 1 (securin)	0.00205	3.81
	1854 at	MYBL2	v-myb myeloblastosis viral oncogene homolog (avian)-like 2	0.00044	3.73
	893 at	UBE2S	ubiquitin-conjugating enzyme E2S	0.00536	3.68
	1651 at	UBE2C	ubiquitin-conjugating enzyme E2C	0.00499	3.66
	36837 at	KIF2C	kinesin family member 2C	0.00074	3.55
14	39109_at	TPX2	TPX2, microtubule-associated protein homolog (Xenopus laevis)	0.00472	3.24
15	40690_at	CKS2	CDC28 protein kinase regulatory subunit 2	0.0017	3.23
16	35995_at	ZWINT	ZW10 interactor	0.00304	3.16
	41583_at	FEN1	flap structure-specific endonuclease I	0.00278	3.02
	35907_at	Cyclin F	cyclin F	0.002	3.01
	34814_at	UBA2	SUMO-1 activating enzyme subunit 2	0.0021	2.96
	34314_at	RRM1	ribonucleotide reductase M1 polypeptide	0.00246	2.94
	32662_at	MDC1	mediator of DNA damage checkpoint 1	0.00042	2.89
	1055_g_at	RFC4	replication factor C (activator 1) 4, 37kDa	0.00082	2.88
	1599_at	CDKN3	cyclin-dependent kinase inhibitor 3 (CDK2-associated dual specificity phosphatase)	0.00234	2.77
	1516_g_at			0.00031	2.75
	32120_at	SPAG5	sperm associated antigen 5	0.00745	2.75
	947_at	MCM7	MCM7 minichromosome maintenance deficient 7 (S. cerevisiae)	0.00535	2.72
	36863_at	HMMR	hyaluronan-mediated motility receptor (RHAMM)	0.00026	2.71
	35844_at 39677 at	SDC4	syndecan 4 (amphiglycan, ryudocan)	0.00212	2.66
	38414 at	KIAA0186 CDC20	KIAA0186 gene product CDC20 cell division cycle 20 homolog (S. cerevisiae)	0.00895 0.00305	2.65
	38804_at	CSE1L	CSE1 chromosome segregation 1-like (yeast)	0.00305	2.64 2.55
	527 at	CENPA	centromere protein A, 17kDa	0.00176	2.52
	39092 at	H2AFV	H2A histone family, member V	0.00173	2.52
	34715 at	FOXM1	forkhead box M1	0.00938	2.51
	36813 at	TRIP13	thyroid hormone receptor interactor 13	0.00045	2.48
	36591 at	TUBA1	tubulin, alpha 1 (testis specific)	0.00661	2.45
	36572 r at	ARL6IP	ADP-ribosylation factor-like 6 interacting protein	0.00401	2.4
	40145 at	TOP2A	topoisomerase (DNA) II alpha 170kDa	0.00587	2.38
	41081 at	BUB1	BUB1 budding uninhibited by benzimidazoles 1 homolog (yeast)	0.00704	2.34
40	40697 at	Cyclin A2	cyclin A2	0.00037	2.32
41	31600_s_at	PMS2L5	postmeiotic segregation increased 2-like 5	0.00436	2.31
42	36833_at	GLA	galactosidase, alpha	0.00109	2.29
	37302_at	CENPF	centromere protein F, 350/400ka (mitosin)	0.00498	2.29
	1721_g_at	MAD2L1	MAD2 mitotic arrest deficient-like 1 (yeast)	0.00365	2.24
	36457_at	GMPS	guanine monphosphate synthetase	0.00955	2.23
	572_at	TTK	protein kinase hMps1	0.00243	2.21
	330_s_at	arinn i i		0.00504	2.21
	37585_at	SNRPA1	small nuclear ribonucleoprotein polypeptide A'	0.00012	2.19
	36968_s_at	EXOSC8	exosome component 8	0.00805	2.12
	1515_at	0-4		0.00692	2.1
	40717_at 37293_at	Cathepsin L2	cathepsin L2 KIAA0097 gene product	0.00017	2.06
	37293_at 37228 at	ch-TOG PLK1	polo-like kinase 1 (Drosophila)	0.00263 0.00314	2.05 2.03
5.4	34880 at	MGC10433	hypothetical protein MGC10433	0.00314	2.03
	36489 at	PRPS1	phosphoribosyl pyrophosphate synthetase 1	0.00855	2.02
	32584 at	PSMD8	proteasome (prosome, macropain) 26S subunit, non-ATPase, 8	0.00833	2.02
	39077 at	DRAP1	DR1-associated protein 1 (negative cofactor 2 alpha)	0.00307	0.43
	37579_at	CYFIP2	cytoplasmic FMR1 interacting protein 2	0.00288	0.41
	36634 at	BTG2	BTG family, member 2	0.00342	0.38
	2020 at	Cyclin D1	cyclin D1 (PRAD1: parathyroid adenomatosis 1)	0.00713	0.36
	1890 at	GDF15	growth differentiation factor 15	0.00621	0.30
	40336 at	FDXR	ferredoxin reductase	0.00288	0.28
	862 at	SERPINB5	serine (or cysteine) proteinase inhibitor, clade B (ovalbumin), member 5	0.00489	0.14
	2031 s at	p21	cyclin-dependent kinase inhibitor 1A (p21, Cip1)	0.00008	0.13

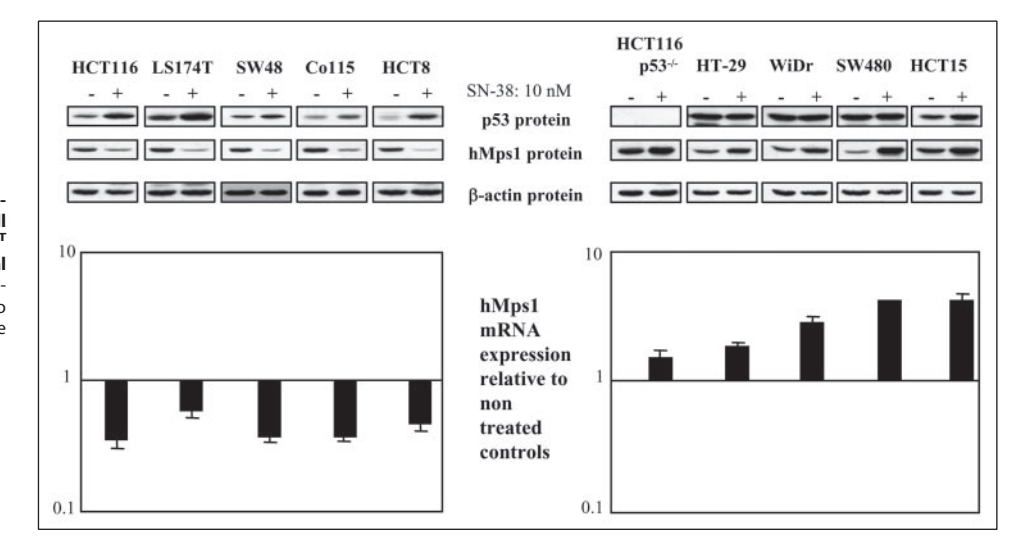


FIGURE 5. Four days after start of SN-38 treatment, p53 protein expression is increased in all p53<sup>WT</sup> cell lines, hMps1 is suppressed in p53<sup>WT</sup> but not in p53-deficient cells as shown by real time RT-PCR and by Western blotting. Expression after treatment relative to expression prior to treatment, determined in real time quantitative PCR, is given as means  $\pm$  S.D.

Overexpression of p53 Leads to Suppression of hMps1 mRNA and Protein—To investigate the regulation of hMps1 by p53, we transduced HCT116p53<sup>-/-</sup> or HCT116p21<sup>WAF1/Cip1-/-</sup> cells with adenoviral vectors expressing wild-type p53 protein or p21 WAF1/Cip1 protein. Additionally, the expression of hMps1 was analyzed in HCT116p21WAF1/Cip1-/- cells after

The reintroduction of p53 protein into p53<sup>-/-</sup> cells up-regulated the p21 WAF1/Cip1 protein expression as expected (Fig. 6A). Additionally, it also down-regulated hMps1 on both mRNA and protein level. Interestingly, the enforced expression of p21 WAF1/Cip1 protein in the absence of p53 had the same effect on expression of hMps1, indicating that high levels of p21 WAF1/Cip1 protein by itself are sufficient to suppress hMps1 mRNA and protein expression (Fig. 6B).

Treatment of HCT116p21WAF1/CIP1-/- cells with SN-38 triggered a moderate up-regulation of p53 protein, but the suppression on mRNA and protein level was negligible (Fig. 6C). These data indicated that the relatively moderate up-regulation of p53 through treatment is not sufficient to suppress hMps1 expression in the absence of p21WAF1/Cip1. Only amounts larger than the physiological amounts of p53 could suppress hMps1 in the absence of p21<sup>WAFI/CIP1</sup> (Fig. 6D and Fig. 7B).

These data suggested that the p53 protein regulates hMps1 mRNA and protein levels and that this effect is modulated by p21WAF1/Cip1. Large amounts of either protein alone can suppress the expression of hMps1. Under conditions of SN-38 treatment, the effect of p53 appeared to be enhanced by the overexpression of p21  $^{\mathrm{WAF1/Cip1}}$  protein.

The p53-mediated Suppression of hMps1 Is Enhanced by p21 $^{WAF1/Cip1}$ — Several authors indicated recently that p21<sup>WAF1/Cip1</sup> protein may play a regulatory role in gene transcription (29, 30). To investigate the role of p21WAF1/Cip1 protein in the p53-mediated suppression of hMps1 in more detail, HCT116 (p21WAF1/Cip1+/+) cells and HCT116p21WAF1/Cip1-/- cells were transduced with variable amounts of adenoviral vector expressing p53<sup>WT</sup> protein or p21<sup>WAF1/Cip1</sup> protein. Dose-response experiments showed that the level of p53 protein achieved at a multiplicity of infection (m.o.i.) of 20 yields a p21 WAF1/Cip1 expression comparable with that obtained after SN-38 treatment (supplemental Fig. S4A).

The transduction with p53-expressing adenoviral vector decreased the expression of hMps1 in the HCT116 cell line in a concentration-dependent manner (Fig. 7, A and D), but there was a very weak suppression of hMps1 in the p21 $^{WAF1/Cip1-/-}$  cell line (Fig. 7, B and E), indicating that p21<sup>WAF1/Cip1</sup> presence is necessary for the suppressive activity of p53. This was evident on mRNA and protein level. In the presence of p21WAF1/Cip1, a concentration-dependent suppression of hMps1

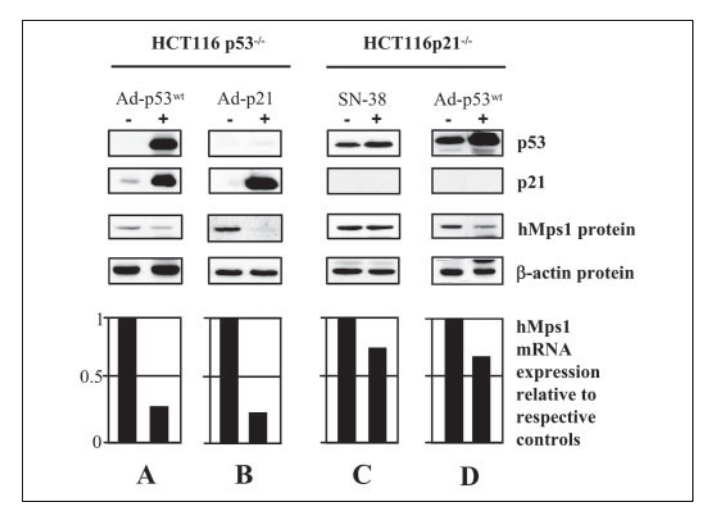


FIGURE 6. hMps1 is suppressed on the mRNA and protein level after overexpression of p53 and p21  $^{\text{WAF1/Cip1}}$  proteins. A, transduction of p53  $^{-/-}$  cells with adenoviral vector coding for p53 protein leads to up-regulation of p21  $^{\text{WAF1/Cip1}}$  and suppression of hMps1 on the transcriptional and protein level. B, transduction with p21WAF1/Cip1-expressing virus in the absence of p53 protein suppresses hMps1. C, treatment of HCT116p21<sup>-/-</sup> cells with SN-38 enhances expression of p53 protein, which in the absence of p21WAF1/Cip1 is not sufficient to suppress hMps1. D, transduction of HCT116p21<sup>-/-</sup> cells with adenoviral vector (m.o.i. = 25) expressing p53 suppresses hMps1. Cells transduced with AdLacZ (lanes denoted –) were used as controls. Expression after treatment relative to expression prior to treatment, determined in real time quantitative PCR, is given as means  $\pm$  S.D. (which were negligible).

protein was visible starting at an m.o.i. of 2.5. By contrast, in the absence of p21WAF1/Cip1, the suppression of hMps1 was seen only at high levels of p53 protein (20 m.o.i.) (Fig. 7B). The expression of exogenous p21 protein alone in HCT116p21WAF1/Cip1-/- cells was sufficient to suppress the hMps1-mRNA and -protein expression (Fig. 7, C and F). Furthermore, the time course of hMps1 suppression in the p53<sup>WT</sup> cells after SN-38 treatment showed that the suppression was strongest about 48 h after start of treatment, and only after p21 protein was strongly overexpressed (supplemental Fig. S4B). This further confirms the importance of p21 in the down-regulation of hMps1.

Suppression of hMps1 Inhibits SN-38-induced Apoptosis in p53<sup>MUT</sup> Cells—To investigate how hMps1 affects the cellular reaction to treatment, HeLa cells were transfected either with pSUPER-EGFP (control) or with pSUPER-hMps1 and treated for 2 and 3 days with SN-38. HeLa



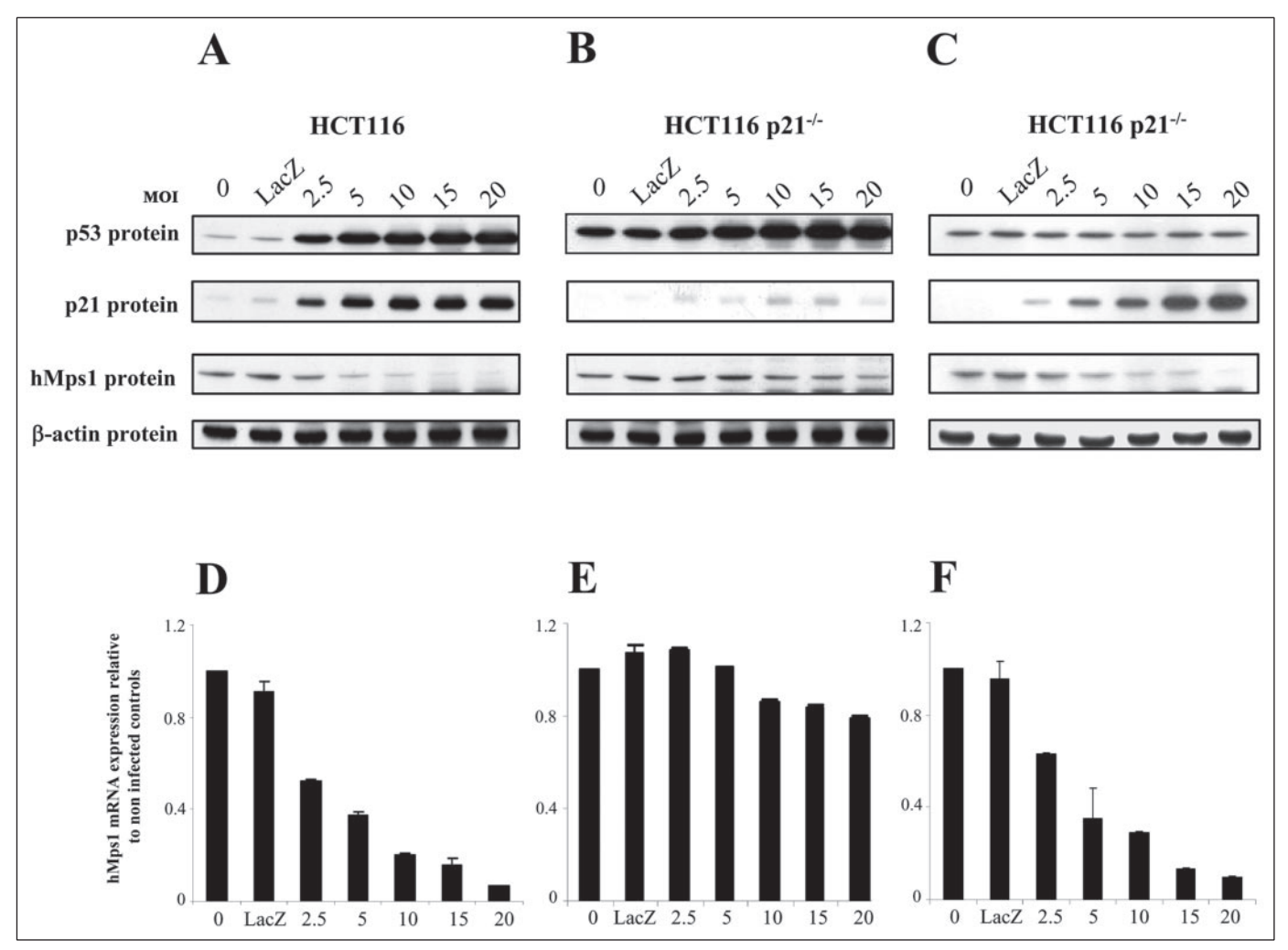


FIGURE 7. **p21**<sup>WAF1/Cip1</sup> is necessary and sufficient for the down-regulation of hMps1. *A*, variable amounts of AdeCMVp53 adenovirus, given as multiplicity of infection (*MOI*) were used for transduction of HCT116 cells or of HCT116p21<sup>WAF1/Cip1-/-</sup> cells (*B*). *C*, HCT116 p21<sup>WAF1/Cip1-/-</sup> cells were tranduced with variable amounts of the AdeCMVp21 adenovirus. *D*, E, and F, relative amounts of hMps1-mRNA, corresponding to the protein amounts shown in A, B, and C, were determined by real time quantitative PCR and are given as means ± S.D.

cells, which are deficient in p53 function (31) and exhibit a very good uptake of the pSUPER-hMps1 plasmid (data not shown), were reported previously to undergo a DNA damage-induced mitotic arrest followed by apoptosis, which was dependent on a functional mitotic checkpoint (32). After almost complete suppression of hMps1, the mitotic checkpoint was abrogated, visible through suppression of phosphorylation of BubR1 and of histone H3 (Fig. 8A) and the decrease of the mitotic fraction at day 2 and day 3 (Fig. 8C). Simultaneously, the percentage of micronucleated cells increased (Fig. 8, B and C), whereas the PARP fragmentation (Fig. 8A) and nuclear condensation (Fig. 8, B and C) decreased. The specificity of the effect of hMPS1 inhibition in the assays was confirmed by the lack of any impact of the transfection with pSU-PER-EGFP or, as two other controls, with pSUPER-hMLH1 (siRNA against a mismatch repair protein) or pSUPER-mCMV56 (siRNA against immediate early protein of mouse cytomegalovirus) (data not shown) on hMps1 expression or extent of apoptosis.

The siRNA-mediated specific suppression of hMps1 in HT-29 cells triggered a similar significant suppression of apoptosis, as measured by PARP cleavage, nuclear condensation, and a decrease in caspase 3 + caspase 7 activity (data not shown).

Inhibition of hMps1 Kinase Activity Suppresses SN-38-induced Apoptosis—We further investigated, how the inhibition of the hMps1 kinase activity affects DNA damage-induced apoptosis. hMps1 kinase activity was specifically suppressed in HCT116p53<sup>-/-</sup> cells by transfection with a dominant-negative kinase-dead mutant of hMps1 (hMps1-KD). Three days after treatment, hMps1-KD expressing cells showed a significantly lower percentage of apoptotic condensed nuclei, concomitant with a higher percentage of micronucleations and interphases (Fig. 9C) than the cells transfected with pcDNA-GFP (Fig. 9A) or with pcDNA-hMps1 plasmid (Fig. 9B).

Collectively, the results presented in Figs. 8 and 9 indicate that the unscheduled expression of hMps1 in the SN-38-treated  $p53^{\mathrm{MUT}}$  cells contributes to their apoptosis. The suppression of hMps1 abrogates the mitotic checkpoint and allows more mitoses to proceed to micronucleation, thus decreasing apoptosis within the time of observation.

#### **DISCUSSION**

p53 Status Determines the Cellular Response to SN-38-We have selected 10 human colon carcinoma cell lines with known p53 status and that behave differently after treatment with SN-38. We show that in response to SN-38-induced DNA damage, both groups of cell lines undergo a transient G<sub>2</sub>/M cell cycle arrest from which the p53<sup>WT</sup> cell lines slip into a long term tetraploid  $G_1$  arrest, as described previously (33). The long term arrest was associated with senescence (data not shown) that was independent of p16 protein expression (Fig. 2). The  $\mathrm{p53^{MUT}}$  cell lines leave the  $\mathrm{G}_{\mathrm{2}}$  phase arrest, enter aberrant mitoses (20 –



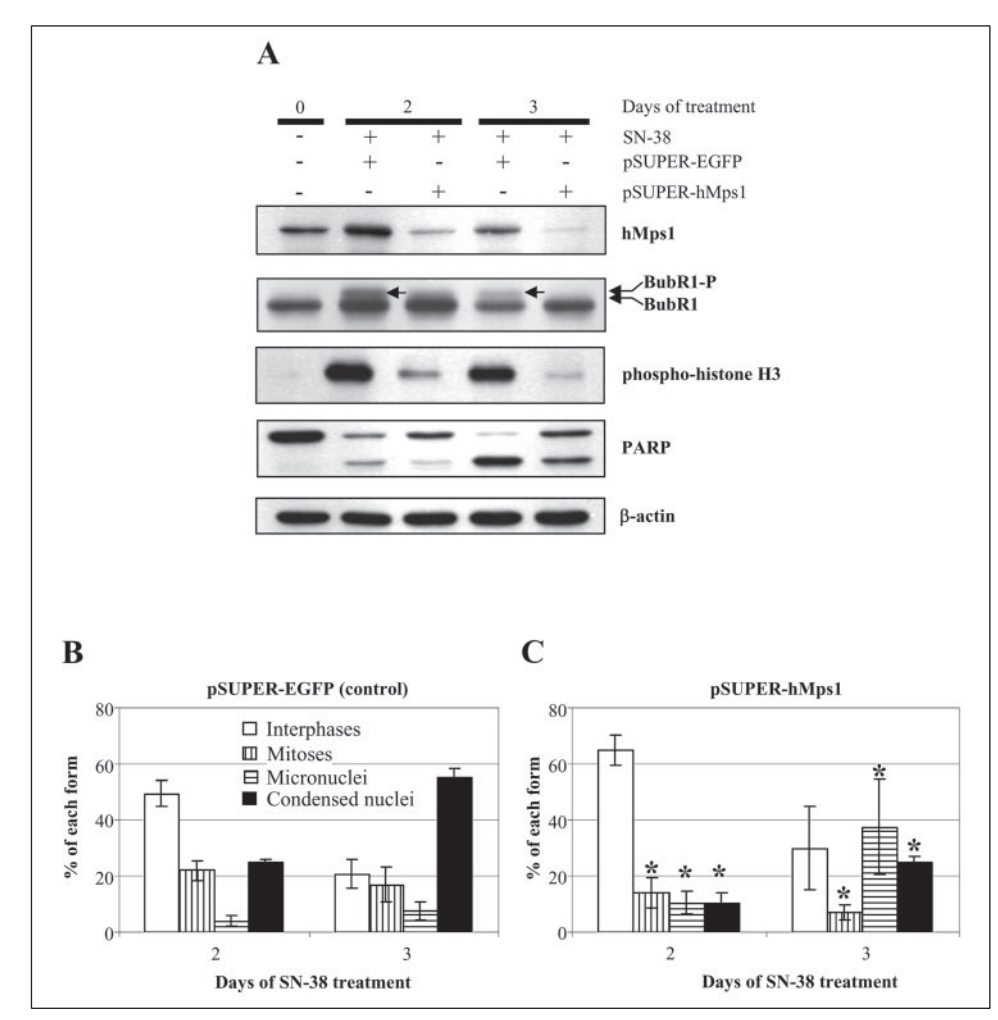


FIGURE 8. Suppression of hMps1 protein abrogates the mitotic checkpoint and inhibits SN-38-induced apoptosis in HeLa cells. Cells were transfected by electroporation either with pSUPER-EGFP or with pSUPER-hMps1 and seeded. The following day, cells were treated with 10 nm SN-38 and harvested for morphological analysis and for Western blot at the indicated time points. A, Western blots show a strong suppression of hMps1 and a concomitant decreases of phosphorylation of BubR1 and of histone H3 and a decrease in the extent of PARP fragmentation. B, pSUPER-EGFP transfected cells show on days 2 and 3 a high percentage of mitoses and condensed nuclei. C, transfection with pSUPER-hMps1 leads to a decrease in the percentage of mitoses and condensed nuclei and to an increase in the percentage of micronuclei at both time points. Means  $\pm$ S.D. are of three independent experiments. Asterisk denotes p < 0.001 as determined by paired t

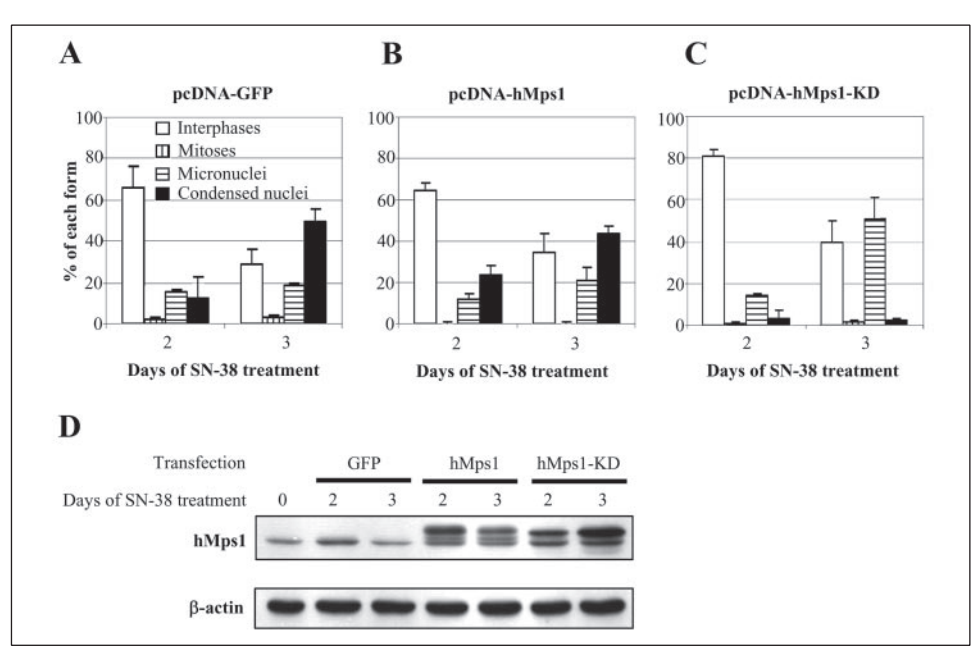


FIGURE 9. Inhibition of hMps1 kinase activity suppresses SN-38-induced apoptosis. HCT116 cells were transfected with pcDNA-GFP, pcDNA-hMps1, or pcDNA-hMps1-KD, and 1 day later they were treated with 10 nm SN-38. At the indicated time points of continuous treatment, the cells were harvested, and the morphologies were evaluated in cytospins after DAPI staining. The transfected cells were identified through GFP protein (control) or by staining with anti-Myc antibody (to detect hMps1 or hMps1-KD). A, pcDNA-GFP transfected HCT116 p53<sup>-/-</sup> cells show a high percentage of condensed nuclei (apoptosis) at 3 days of treatment. B, transfection with hMps1 plasmid has no effect on apoptosis. C, pcDNA-hMps1-KD transfected cells show significantly less condensed nuclei and more micronucleations and interphases at the same time point. D, Western blot showing the expression of endogenous and exogenous hMps1 protein (wild-type and kinase-dead) in each experiment. The shift of the upper band of the exogenous hMps1 was postulated to be due to the autophosphorylation (20).

30% as analyzed by phosphohistone H3 staining at 48 h; data not shown), and finally undergo apoptosis. Similar dependence of the type of cellular response to DNA damage on the p53 status has been observed previously in single cell lines derived from colon carcinoma (1, 34, 35), glioblastoma (36), and breast carcinoma (37).

Apoptosis-associated Expression Profile of p53-defective Cell Lines Defined—There was a consistent association of the presence of a nonfunctional p53 protein with apoptosis, making it possible to detect gene alterations preceding or involved in this process. We analyzed the ratio of gene expression in  $p53^{\mathrm{MUT}}$  to  $p53^{\mathrm{WT}}$  cell lines prior to and after

treatment (supplemental Fig. 3A). The change of this ratio clearly showed that generally the p53-dependent basal differences (prior to treatment) are strongly enhanced after treatment-induced overexpression of p53. The analysis prior to treatment did not identify significant differences in gene expression between the two groups, *i.e.* the basal profiles were not suitable for prediction of the reaction to DNA damage.

New Genes Regulated by p53 Identified—The hierarchical gene clustering showed directly the inverse relationship between the gene expression in p53  $^{\rm WT}$  and p53  $^{\rm MUT}$  cell lines after treatment (supplemental Fig. 3B). We identified a number of genes involved in mitosis regulation that appear to be transcriptionally suppressed by p53, e.g. TTK/hMps1, KNTC2/Hec1, BUB1, K1F2C, CDC20, CENPA, CENPF, and PLK1. Most of them were not known as p53 targets and extend the previously described family of p53-suppressible genes regulating  $\rm G_2/M$  arrest and mitosis (38–44). It appears likely that the coordinate suppression of mitotic genes by p53 is an additional safeguard mechanism protecting cells from entering mitosis after DNA damage. Indeed, we found that the suppression of p53 protein in SN-38 treated HCT116 cells leads to an increase in hMps1 expression (supplemental Fig. S5) and to a decrease of tetraploid arrest and an increase of apoptosis (2). This indicates that p53 is a part of a regulatory link between DNA damage and mitosis.

p21 Plays a Role in Transcriptional Regulation-Notably, we found an enhancement of the transcriptional suppression of hMps1 by p21 WAF1/Cip1, thus extending previous reports on the transcriptional down-regulation of mitotic checkpoint genes by p21<sup>WAF1/Cip1</sup> (29, 30). The involvement of p21 $^{\text{WAF1/Cip1}}$  was not merely dependent on the  $G_1$ arrest, because the induction of G<sub>1</sub> arrest by serum starvation did not induce suppression (data not shown). Overexpression of p21WAF1/Cip1 may lead to the inhibition of cyclin-dependent kinases, which stabilizes the pRb-E2F complex and prevents E2F activity. Under such circumstances, E2F has been shown to play a role as a transcriptional repressor (45). Indeed, E2F-binding sites have been found in the promoter of hMps1 (46). Alternatively, both p53 and p21WAF1/Cip1 are capable of binding to the CDE/CHR element in the promoter of cell cycle regulatory genes (41, 47). Whether these elements are present in the promoter of hMps1 and other identified mitosis-regulating genes remains to be determined; the present results are consistent with either model.

The Role of hMps1 in Apoptosis Induction—The lack of p53-mediated transcriptional down-regulation after DNA damage in the p53-deficient cell lines leads to an unscheduled gene expression; 16 mitosis-related genes, including hMps1, are strongly expressed after damage.

The intact mitotic checkpoint has been shown recently to be necessary for DNA damage-induced apoptosis; its abrogation by an inhibitor (48) or by suppression of the proteins BubR1 or Mad2 (32) decreased the frequency of mitotic cell death after DNA damage. Also during the activation of the mitotic checkpoint by nocodazole, the ectopic overexpression of BubR1 increases the death of polyploid cells (49). Furthermore, cells in which mitotic checkpoint genes, *e.g. BUBR1, MAD2* (32), or *TTK*/hMps1 (20), are suppressed after microtubular damage show a nonapoptotic transformation of the nucleus. These data as well as the present results indicate that the levels of the mitotic checkpoint proteins control the course of transformation of aberrant mitoses into apoptotic, condensed nuclei or nonapoptotic nuclear forms (Fig. 10).

A damage sensor function independent from the mitotic checkpoint function has been proposed recently for hMps1 by Wei *et al.* (50). The authors postulated a cross-talk between the mitotic checkpoint and the DNA damage checkpoint through hMps1-mediated phosphorylation of the Chk2 kinase. After SN-38 treatment, however, we found Chk2 phosphorylation in HCT116p53 $^{-/-}$  as well as in HCT116 cells (data not shown), in which hMps1 is suppressed following DNA damage (Fig. 5),

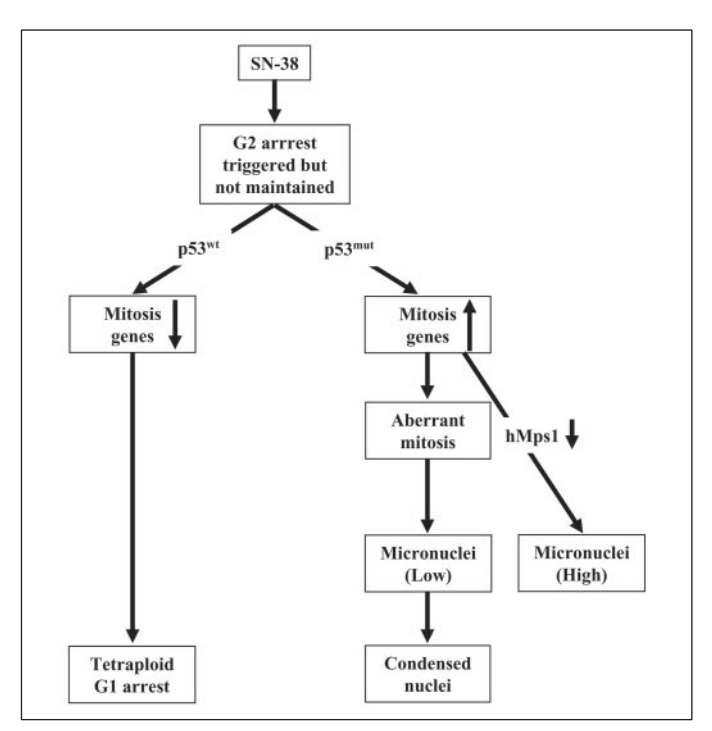


FIGURE 10. SN-38 treatment of colon carcinoma cells induces an initial  $G_2/M$  arrest which is independent from the p53 status. The p53-mediated suppression of mitotic genes, including hMps1, in p53 $^{WT}$  cells is associated with the transition into a tetraploid  $G_1$  arrest. The lack of this suppression in p53 $^{MUT}$  cells allows mitotic entry, which eventually leads to apoptotic nuclear condensation. Suppression/inhibition of the hMps1 kinase abrogates the mitotic checkpoint that leads to a higher number of micronucleated cells. For clarity, some pathways of nuclear transformation (interphases into condensed nuclei or micronuclei) have been omitted.

indicating that at least in the present system Chk2 can be phosphorylated also in the absence of hMps1.

In conclusion, the present data support the notion that mitotic checkpoint proteins, here represented by hMps1, contribute to apoptosis of p53<sup>MUT</sup> cells after DNA damage. The exact signaling mechanism is not known at present. Its pharmacological enhancement should potentiate apoptosis after chemotherapy in the p53<sup>MUT</sup> cells but not in p53<sup>WT</sup> cells and enable selective killing of tumor cells.

Acknowledgments—SN-38 was a kind gift from Agnes Gonthier, Aventis Pharma S.A., Vitry-sur-Seine, Cedex, France. The cell lines HCT116p53<sup>-/-</sup> and HCT116p21<sup>-/-</sup> were a kind gift of Dr. Bert Vogelstein (Howard Hughes Medical Institute and The Sidney Kimmel Comprehensive Cancer Center, The Johns Hopkins University Medical Institutions, Baltimore). We acknowledge the perfect technical assistance provided by Britta Jebautzke, and we thank Dr. Erich Nigg for hMps1 plasmids and helpful comments and suggestions. We also thank Dr. Jürgen Behrens for critical reading of the manuscript.

#### REFERENCES

- Magrini, R., Bhonde, M. R., Hanski, M. L., Notter, M., Scherubl, H., Boland, C. R., Zeitz, M., and Hanski, C. (2002) Int. I. Cancer 101, 23–31
- Bhonde, M. R., Hanski, M. L., Notter, M., Gillissen, B. F., Daniel, P. T., Zeitz, M., and Hanski, C. (2006) Oncogene 25, 165–175
- 3. Yu, J., and Zhang, L. (2005) Biochem. Biophys. Res. Commun. 331, 851-858
- 4. Roninson, I. B., Broude, E. V., and Chang, B. D. (2001) Drug Resist. Updat. 4, 303–313
- Sato, N., Mizumoto, K., Nakamura, M., Ueno, H., Minamishima, Y. A., Farber, J. L., and Tanaka, M. (2000) Oncogene 19, 5281–5290
- Castedo, M., Perfettini, J. L., Roumier, T., Valent, A., Raslova, H., Yakushijin, K., Horne, D., Feunteun, J., Lenoir, G., Medema, R., Vainchenker, W., and Kroemer, G. (2004) Oncogene 23, 4362–4370
- Chen, Z., Xiao, Z., Chen, J., Ng, S. C., Sowin, T., Sham, H., Rosenberg, S., Fesik, S., and Zhang, H. (2003) Mol. Cancer Ther. 2, 543–548
- 8. Liu, Q., Guntuku, S., Cui, X. S., Matsuoka, S., Cortez, D., Tamai, K., Luo, G., Carattini-



- Rivera, S., DeMayo, F., Bradley, A., Donehower, L. A., and Elledge, S. J. (2000) Genes Dev. 14, 1448-1459
- Chan, T. A., Hwang, P. M., Hermeking, H., Kinzler, K. W., and Vogelstein, B. (2000) Genes Dev. 14, 1584-1588
- 10. Chan, T. A., Hermeking, H., Lengauer, C., Kinzler, K. W., and Vogelstein, B. (1999) Nature 401, 616-620
- 11. Tu, S. P., Jiang, X. H., Lin, M. C., Cui, J. T., Yang, Y., Lum, C. T., Zou, B., Zhu, Y. B., Jiang, S. H., Wong, W. M., Chan, A. O., Yuen, M. F., Lam, S. K., Kung, H. F., and Wong, B. C. (2003) Cancer Res. 63, 7724-7732
- 12. Sihn, C. R., Suh, E. J., Lee, K. H., Kim, T. Y., and Kim, S. H. (2003) Cancer Lett. 201,
- 13. Cogswell, J. P., Brown, C. E., Bisi, J. E., and Neill, S. D. (2000) Cell Growth & Differ. 11, 615-623
- 14. Burns, T. F., Fei, P., Scata, K. A., Dicker, D. T., and El-Deiry, W. S. (2003) Mol. Cell. Biol. 23, 5556-5571
- 15. Lock, R. B., and Stribinskiene, L. (1996) Cancer Res. 56, 4006 4012
- 16. Nabha, S. M., Mohammad, R. M., Dandashi, M. H., Coupaye-Gerard, B., Aboukameel, A., Pettit, G. R., and Al-Katib, A. M. (2002) Clin. Cancer Res. 8, 2735-2741
- 17. Martin-Lluesma, S., Stucke, V. M., and Nigg, E. A. (2002) Science 297, 2267–2270
- 18. Liu, S. T., Chan, G. K., Hittle, J. C., Fujii, G., Lees, E., and Yen, T. J. (2003) Mol. Biol. Cell 14, 1638-1651
- 19. Nigg, E. A. (2001) Nat. Rev. Mol. Cell. Biol. 2, 21-32
- 20. Stucke, V. M., Sillje, H. H., Arnaud, L., and Nigg, E. A. (2002) EMBO J. 21, 1723-1732
- 21. Sato, S., Fujita, N., and Tsuruo, T. (2002) Oncogene 21, 1727-1738
- 22. Bhonde, M. R., Hanski, M. L., Magrini, R., Moorthy, D., Muller, A., Sausville, E. A., Kohno, K., Wiegand, P., Daniel, P. T., Zeitz, M., and Hanski, C. (2005) Oncogene 24,
- 23. Ihaka, R., and Gentleman, R. (1996) J. Comput. Graphical Statistics 5, 299-314
- 24. Irizarry, R. A., Bolstad, B. M., Collin, F., Cope, L. M., Hobbs, B., and Speed, T. P. (2003) Nucleic Acids Res. 31, e15
- 25. Irizarry, R. A., Hobbs, B., Collin, F., Beazer-Barclay, Y. D., Antonellis, K. J., Scherf, U., and Speed, T. P. (2003) Biostatistics 4, 249-264
- 26. Cleveland, W. (1979) J. Am. Stat. Assoc. 74, 829 836
- 27. Eisen, M. B., Spellman, P. T., Brown, P. O., and Botstein, D. (1998) Proc. Natl. Acad. Sci. U. S. A. **95,** 14863–14868
- 28. Hemmati, P. G., Gillissen, B., von Haefen, C., Wendt, J., Starck, L., Guner, D., Dorken, B., and Daniel, P. T. (2002) Oncogene 21, 3149-3161
- 29. Chang, B. D., Broude, E. V., Fang, J., Kalinichenko, T. V., Abdryashitov, R., Poole, J. C., and Roninson, I. B. (2000) Oncogene 19, 2165-2170
- 30. Lohr, K., Moritz, C., Contente, A., and Dobbelstein, M. (2003) J. Biol. Chem. 278,

- 32507-32516
- 31. Scheffner, M., Munger, K., Byrne, J. C., and Howley, P. M. (1991) Proc. Natl. Acad. Sci. U. S. A. 88, 5523-5527
- 32. Nitta, M., Kobayashi, O., Honda, S., Hirota, T., Kuninaka, S., Marumoto, T., Ushio, Y., and Saya, H. (2004) Oncogene 23, 6548 - 6558
- 33. Andreassen, P. R., Lacroix, F. B., Lohez, O. D., and Margolis, R. L. (2001) Cancer Res. **61**, 7660 – 7668
- Bunz, F., Dutriaux, A., Lengauer, C., Waldman, T., Zhou, S., Brown, J. P., Sedivy, J. M., 34. Kinzler, K. W., and Vogelstein, B. (1998) Science 282, 1497-1501
- 35. te Poele, R. H., and Joel, S. P. (1999) Br. J. Cancer 81, 1285-1293
- 36. Wang, Y., Zhu, S., Cloughesy, T. F., Liau, L. M., and Mischel, P. S. (2004) Oncogene 23, 1283-1290
- 37. Hattangadi, D. K., DeMasters, G. A., Walker, T. D., Jones, K. R., Di, X., Newsham, I. F., and Gewirtz, D. A. (2004) Biochem. Pharmacol. 68, 1699-1708
- 38. Krause, K., Wasner, M., Reinhard, W., Haugwitz, U., Dohna, C. L., Mossner, J., and Engeland, K. (2000) Nucleic Acids Res. 28, 4410 - 4418
- 39. Yun, J., Chae, H. D., Choy, H. E., Chung, J., Yoo, H. S., Han, M. H., and Shin, D. Y. (1999) J. Biol. Chem. 274, 29677–29682
- 40. Hoffman, W. H., Biade, S., Zilfou, J. T., Chen, J., and Murphy, M. (2002) J. Biol. Chem. 277, 3247-3257
- 41. St Clair, S., Giono, L., Varmeh-Ziaie, S., Resnick-Silverman, L., Liu, W. J., Padi, A., Dastidar, J., DaCosta, A., Mattia, M., and Manfredi, J. J. (2004) Mol. Cell 16, 725-736
- 42. Chun, A. C., and Jin, D. Y. (2003) J. Biol. Chem. 278, 37439 -37450
- 43. Zhou, Y., Gwadry, F. G., Reinhold, W. C., Miller, L. D., Smith, L. H., Scherf, U., Liu, E. T., Kohn, K. W., Pommier, Y., and Weinstein, J. N. (2002) Cancer Res. 62,
- 44. Mirza, A., Wu, Q., Wang, L., McClanahan, T., Bishop, W. R., Gheyas, F., Ding, W., Hutchins, B., Hockenberry, T., Kirschmeier, P., Greene, J. R., and Liu, S. (2003) Oncogene 22, 3645-3654
- 45. Muller, H., and Helin, K. (2000) Biochim. Biophys. Acta 1470, M1-M12
- 46. Semizarov, D., Kroeger, P., and Fesik, S. (2004) Nucleic Acids Res. 32, 3836-3845
- 47. Taylor, W. R., and Stark, G. R. (2001) Oncogene 20, 1803-1815
- 48. Vogel, C., Kienitz, A., Muller, R., and Bastians, H. (2004) J. Biol. Chem. 280, 4025 - 4028
- 49. Shin, H. J., Baek, K. H., Jeon, A. H., Park, M. T., Lee, S. J., Kang, C. M., Lee, H. S., Yoo, S. H., Chung, D. H., Sung, Y. C., McKeon, F., and Lee, C. W. (2003) Cancer Cell 4,
- 50. Wei, J. H., Chou, Y. F., Ou, Y. H., Yeh, Y. H., Tyan, S. W., Sun, T. P., Shen, C. Y., and Shieh, S. Y. (2005) J. Biol. Chem. 280, 7748-7757



# **Supplemental Data**

**Table S1**. Genes whose expression was tested in semiquantitative RT-PCR, primers and conditions used.

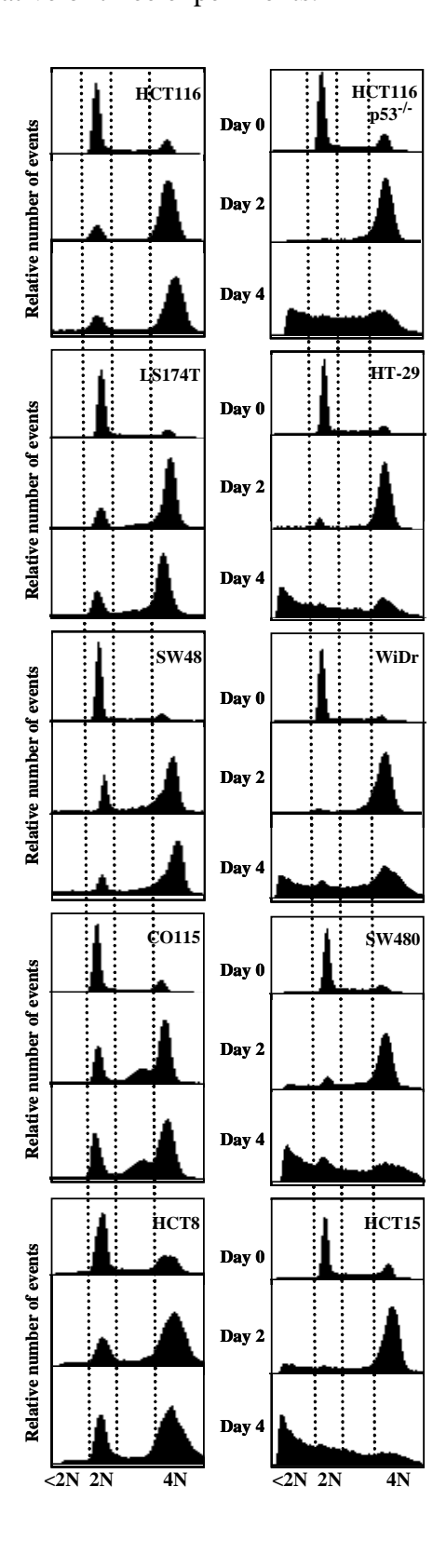
Gene symbol	Description		Primer sequence	PCR conditions	
Amphiregulin	Amphiregulin	F	CATTATGCTGCTGGATTGGA	95°C 10min, 94°C 1min, 60°C 1min, 72°C 1min. 72°C 7min	
Ampiniegumi	Anphileguin	R	TCATGGACTTTTCCCCACAC	93 C 1011mi, 94 C 111mi, 00 C 111mi, 72 C 111mi. 72 C 711mi	
APRIL	Acidic protein rich in leucines	F R	TGCCCCAGCTTACCTACTTG	95°C 10min, 94°C 1min, 60°C 1min, 72°C 1min. 72°C 7min	
	reduce protein remain educes		AATCCATGAGCAGTCCAACC	, , , , , , , , , , , , , , , , , , , ,	
ASNS	Asparagine synthetase	F R	AGCGCCTTGATCGAGTACT	95°C 10min, 94°C 1min, 58°C 45sec, 72°C 45sec. 72°C 7min	
		F	TGACTTGTAGTGGGTCAGCG AACAGGCCACCACATACCTC		
BTG2	B-cell translocation gene 2	R	CTCTGCCCAGGACCTCATTA	95°C 10min, 94°C 1min, 60°C 1min, 72°C 1min. 72°C 7min	
2011/100		F	CTGGAGTACCGGTTCTACAA	0.000.00.00.00.00.00.00.00.00.00.00.00.	
CSNK1G2	casein kinase I gamma 2	R	GATGATGTGGATGGCATGCT	95°C 10min, 94°C 1min, 57°C 1min, 72°C 1min. 72°C 7min	
Cyclin D1	Cyclin D1	F	AGGTCTGCGAGGAACAGAAG	95°C 10min, 94°C 1min, 60°C 1min, 72°C 1min. 72°C 7min	
усшт Бт	Cyclin D1		AGCGTGTGAGGCGGTAGTAG	93 C 1011mi, 94 C 111mi, 60 C 111mi, 72 C 111mi. 72 C 711mi	
Cyr61	Cysteine-rich protein 61		GAAAGTTTCCAGCCCAACTG	95°C 10min, 94°C 1min, 60°C 1min, 72°C 1min. 72°C 7min	
-,		R F	TACACTGGCTGTCCACAAGG	, , , , , , , , , , , , , , , , , , ,	
FHL2	Four and a half LIM only protein 2  Growth arrest and DNA damage inducibe gene		CGG CTG TGA CTG CAA GGA CTT	95°C 10min, 94°C 30sec, 58°C 30sec, 72°C 1min. 72°C 7min	
			AGC AGT CGT TAT GCC ACT GCC CACTGCAAGGTTCTGATAAG		
GADD 34			GTGTGCCTTTTCCTCCTTCT	95°C 10min, 94°C 45sec, 60°C 45sec, 72°C 1min. 72°C 7min	
	Growth arrest and DNA damage inducibe gene		ACACTGTCCAGCTGGGAGCT		
GADD153			GGGACTGATGCTCCCAATTG	95°C 10min, 94°C 1.5min, 66°C 1.5min, 72°C 1min. 72°C 7min	
CALC1	, and the second	R F	TCTGGTCGCCAGCAACCTGAATCTC	05°C 10min 04°C 45c 60°C 45 70°C 1 70°C 5	
GALS1	Lectin, β galactoside binding	R	CGCCGTCCTTGCTGTGCACACGAT	95°C 10min, 94°C 45sec, 60°C 45sec, 72°C 1min. 72°C 7min	
Hec1	HEC (Highly expressed in cancer)		TCCTCATACATGGCCTCACA	95°C 10min, 94°C 45sec, 60°C 45sec, 72°C 1min. 72°C 7min	
		R F	TGTTCAGCTTCCAGGTCCTT	7. 2. 3. 1.	
HR23A	Human homologue of yeast		GCAAGATCTTGAGTGACGAT	95°C 10min, 94°C 1min, 60°C 1min, 72°C 1min. 72°C 7min	
	RAD23	R F	TTCAGCATCTGGATGAACTG		
Histone H1x	Histone H1x	r R	TCTTGCTACCATGTCCGTG AGCGCCTTGATCGAGTACT	95°C 10min, 94°C 1min, 60°C 1min, 72°C 1min. 72°C 7min	
		F	CCGATATTCCAGAGAAAGATCTTCA		
Mps1	hMps1 protein kinase		TGCTGATAACACTTCAGAGTGATGT	95°C 10min, 94°C 45sec, 60°C 45sec, 72°C 1min. 72°C 7min	
EVEN 61	Interferon inducible transmembrane	F	TTCCCCAAAGCCAGAAGATGCACAA	0500 10 : 0400 45	
FITM1	protein 1	R	CAGGTGTGTGGGTATAAACTGT	95°C 10min, 94°C 45sec, 60°C 45sec, 72°C 1min. 72°C 7min	
Maspin	Maspin (Serine protease inhibitor)	F	CCCTATGCAAAGGAATTGGA	95°C 10min, 94°C 1min, 60°C 1min, 72°C 1min. 72°C 7min	
viaspin		R	CAAGCCTGTGGACTCATCCT	75 C Tollini, 74 C Trimi, 60 C Trimi, 72 C Trimi. 72 C Trimi	
mSHMT2	mitochondrial serine		GTTAAGGAGGAGAGTGAGCT	95°C 10min, 94°C 1min, 60°C 1min, 72°C 1min. 72°C 7min	
	hydroxymethyltransferase gene	R F	GGAGAACTCTCACAGACTGG	<u> </u>	
Myt1	Protein kinase	r R	AGCAGCTTCTCCAGCAACTGG CAGAGAAGACCATGGGAGTTCC	95°C 10min, 94°C 1min, 60°C 1min, 72°C 1min. 72°C 7min	
			CAG GAA AAG GAC CAG CTC AG		
Optineurin	Optineurin	F R	GCC TCC TTG AGT GCA ACT TC	95°C 10min, 94°C 1min, 60°C 1min, 72°C 1min. 72°C 7min	
	CDV . LT.	F	ACTGTGATGCGCTAATGGC	0.000.00.00.00.00.00.00.00.00.00.00.00.	
21	CDK inhibitor	R	ATGGTCTTCCTCTGCTGTCC	95°C 10min, 94°C 1min, 60°C 1min, 72°C 1min. 72°C 7min	
PHGDH	Phosphoglycerate dehydrogenase	F	GGCTCAATGGAGCTGTCTTC	95°C 10min, 94°C 1min, 58°C 45sec, 72°C 45sec. 72°C 7min	
HODII	1 nosphogrycerate denydrogenase	R	TTCAGTCACATGCTGCTTCC	93 C Tollini, 94 C Thini, 38 C 43sec, 72 C 43sec. 72 C 7hini	
PLP2	Proteolipid protein 2	F R	TATGCCTGGTGATCCTGATC	95°C 10min, 94°C 1min, 60°C 1min, 72°C 1min. 72°C 7min	
	1 1		CCTCTCTCAACAAGGACACA	, , , , , , , , , , , , , , , , , , ,	
PYCR1	Pyrroline-5-carboxylate reductase	F	CCTGAGAGCAAAGGTCAAGG GACAGAACTGATAGCACCCTCC	95°C 10min, 94°C 1min, 60°C 45sec, 72°C 45sec. 72°C 7min	
	1	R F	CATCCAGGAGATCCAGGAGC		
RhoGDI	Rho GDP dissociation inhibitor	R	GACTTGATGCTGTAGCTGCC	95°C 10min, 94°C 1min, 62°C 1min, 72°C 1min. 72°C 7min	
		F	TGCTTGAGGAATGAAGACCT		
SLC7A5	Solute carrier family 7, member 5	R	TCCTGGATTCACACAGCAA	95°C 10min, 94°C 1min, 60°C 1min, 72°C 1min. 72°C 7min	
2	o2 minus alabadia	F	CATGGAGGTTTGAAGATGCC	05°C 10min 04°C 1min 60°C 1min 72°C 1min 72°C 7min	
32 microglobulin	β2 microglobulin	R	TGGAGCAACCTGCTCAGATACA	95°C 10min, 94°C 1min, 60°C 1min, 72°C 1min. 72°C 7min	
STAT1	Signal Transducers and activators	F	CAGATGTCTATGATCATTTAC	95°C 10min, 94°C 1min, 52°C 1min, 72°C 1min. 72°C 7min	
	of transcription protein 1	R	CAGTGACATTCAGCAACTCTA		
Syndecan 4	Syndecan 4	F	TCGATCCGAGAGACTGAGT	95°C 10min, 94°C 1min, 60°C 1min, 72°C 1min. 72°C 7min	
	Tumor necrosis factor-related	R F	GGTTTCTTGCCCAGGTCATA  TGCAGAAAGCACAGAAAGGA		
NFRSF6	apoptosis-inducing ligand-receptor		TGCAGAAAGCACAGAAAGGA CCATTCTTTCGAACAAAGCC	95°C 10min, 94°C 1min, 58°C 1min, 72°C 1min. 72°C 7min	
		F	GACCCAGTGATTGAACAAGCATCC		
ГОВ	Transducer of ErbB-2	R	GCCCATACAGAGAGTGCATTGAG	95°C 10min, 94°C 1min, 62°C 1min, 72°C 1min. 72°C 7min	
m	Tumor necrosis factor receptor	F	GGGAGCCGCTCATGAGGAAGTT	2507.40	
ΓRAIL R2	superfamily, member 6		CTGGGTGATGTTGGATGGGAGAGT	95°C 10min, 94°C 45sec, 60°C 45sec, 72°C 1min. 72°C 7min	
CD A D1	Human tumor necrosis factor type	R F	GGAGATTCACTTGCAGACCA	05°C 10min 04°C 1min 60°C 1min 70°C 1min 70°C 7	
TRAP1	1 receptor associated protein	R	CGTAGAAGATGCTGCGGATG	95°C 10min, 94°C 1min, 60°C 1min, 72°C 1min. 72°C 7min	
ΓYRO3	Protein tyrosine kinase	F	CACTGAGCTGGCTGACTAAGCCCC	95°C 10min, 94°C 1min, 58°C 1min, 72°C 1.5min. 72°C 7min	
. 1103	1 TOGET LYTOSHK KHRISE	R	AATGCATGCACTTAAGCAGCAGGG	75 C 1011mi, 77 C 111mi, 50 C 111mi, 72 C 1.511mi. 72 C /11mi	

Table S2  $\label{eq:s2} Analysis \ of \ mitotic \ arrest \ in \ p53-deficient \ cells \ after \ treatment \ with \ 200 \ ng/ml \ (666 \ nM)$  Nocodazole for 16 h

Cell line	% mitoses after Nocodazole treatment
HCT116p53 <sup>-/-</sup>	85
HT-29	74
SW480	40
WiDr	73
HCT-15	77

# **Supplementary figure S1**

SN-38 treatment induces long-term arrest or apoptosis in colon carcinoma cell lines. Histograms of p53<sup>wt</sup> cell lines (left panel) and p53<sup>mut</sup> cell lines (right panel) 0, 2 and 4 days after start of treatment. The tetraploid cell cycle arrest is maintained between 2 and 4 days after start of treatment in cell lines with intact p53. Cells with a deficient or mutated p53 do not maintain the tetraploid cell cycle arrest. Additionally, they also undergo apoptosis (subG1 peak). Results representative of three experiments.

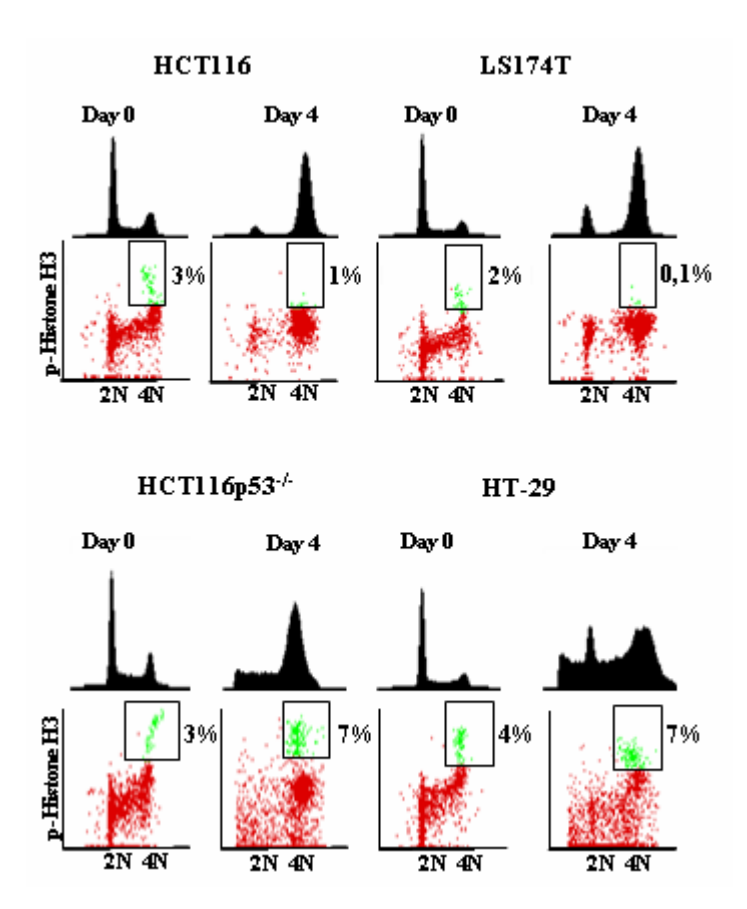


### **Supplementary figure S2**

Analysis of histone H3 phosphorylation in non treated and SN-38 treated p53<sup>wt</sup> and p53-deficient cell lines. Only adherent cells were used for the analysis.

The p53<sup>wt</sup> cell lines (represented here by HCT116 and LS174T) show a lower percentage of phospho-histone H3 as compared to the non treated cells indicating that they are not in the M-phase of the cell cycle.

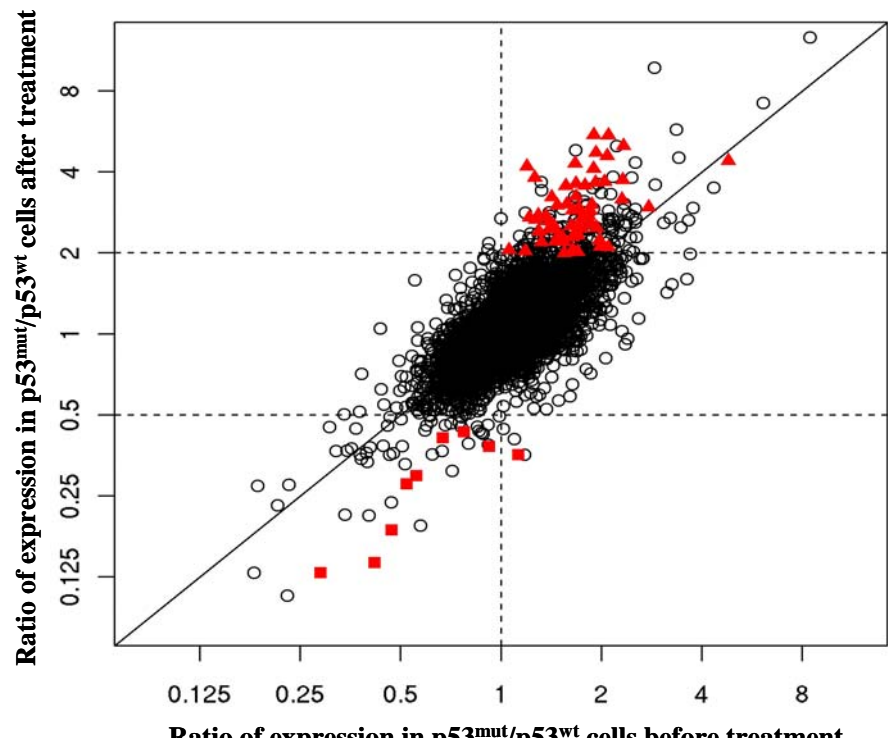
The p53-deficient cell lines (represented here by HCT116p53<sup>-/-</sup> and HT-29) show a higher percentage of phospho-histone H3 positive cells as compared to the non treated cells indicating that the fraction of mitotic cells increases after treatment.



# Supplementary figure S3A

The ratio of expression in p53<sup>mut</sup>/p53<sup>wt</sup> cell lines 4 days after SN-38 treatment, plotted as a function of the ratio of expression in p53<sup>mut</sup>/p53<sup>wt</sup> cell lines before treatment.

The horizontal lines mark the threshold values of twofold change after treatment. The vertical line separates the genes whose ratio of expression in  $p53^{mut}/p53^{wt}$  is <1 or >1 in the basal state. The diagonal separates the genes whose ratio of expression in p53<sup>mut</sup>/p53<sup>wt</sup> before treatment < or > than the ratio p53<sup>mut</sup>/p53<sup>wt</sup> after treatment. Red triangles and red squares indicate the genes listed in the Table I with ratio of expression greater than 2 (triangles) or smaller than 0.5 (squares).

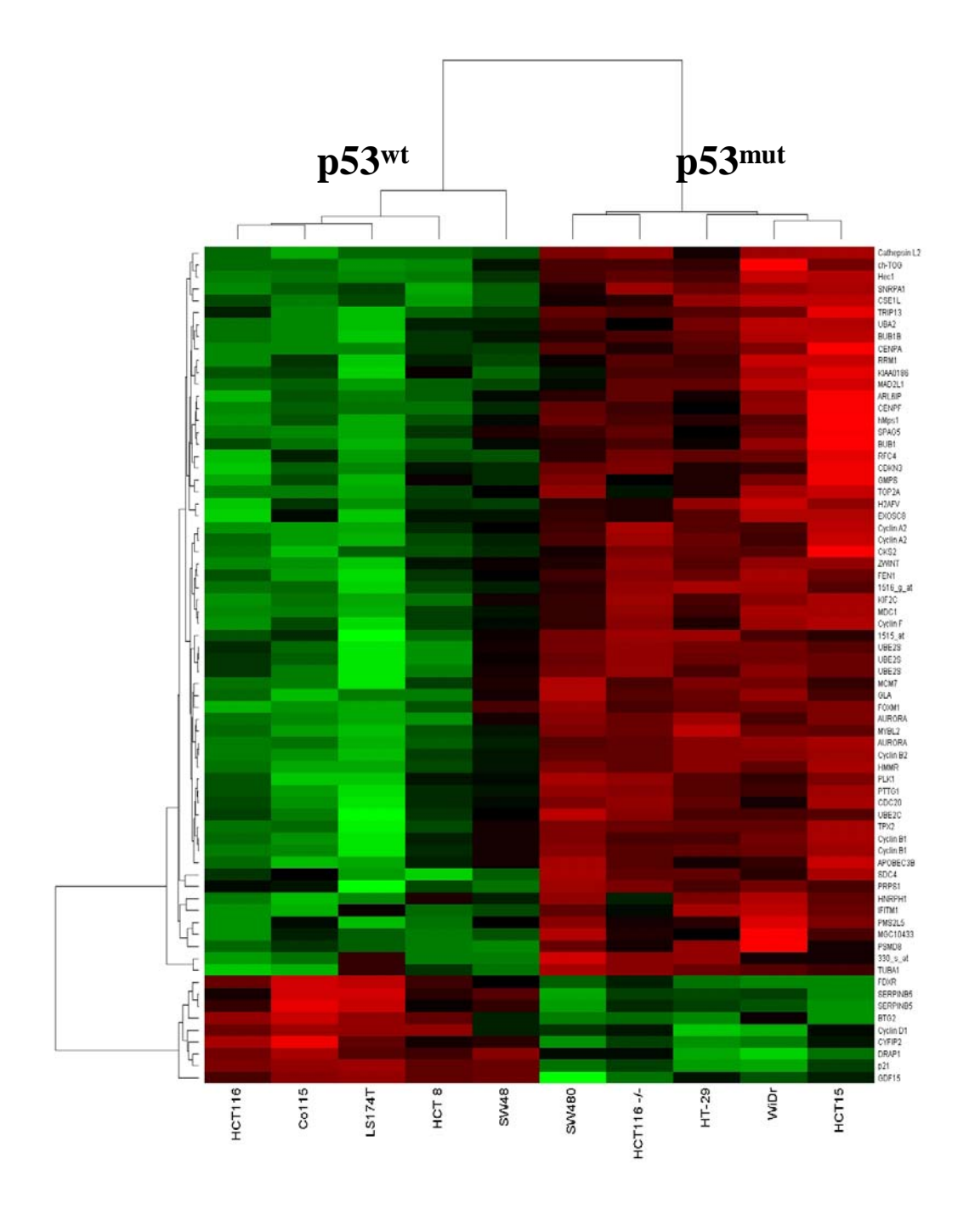


Ratio of expression in p53<sup>mut</sup>/p53<sup>wt</sup> cells before treatment

# **Supplementary figure S3B**

Hierarchical clustering of treatment-induced alterations of genes listed in Table I. Green coloring indicates expression values below the mean expression, red coloring indicates expression values above the mean expression and black color indicates the mean expression

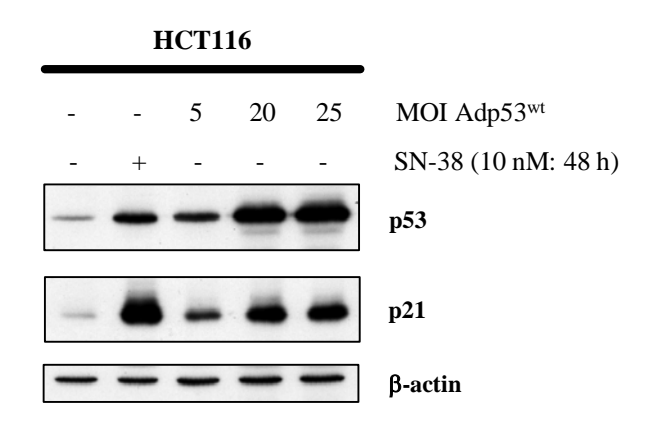
expression values above the mean expression and black color indicates the mean exafter treatment. Names of the 10 cell lines used are given below the diagram.



#### **Supplementary figure S4A**

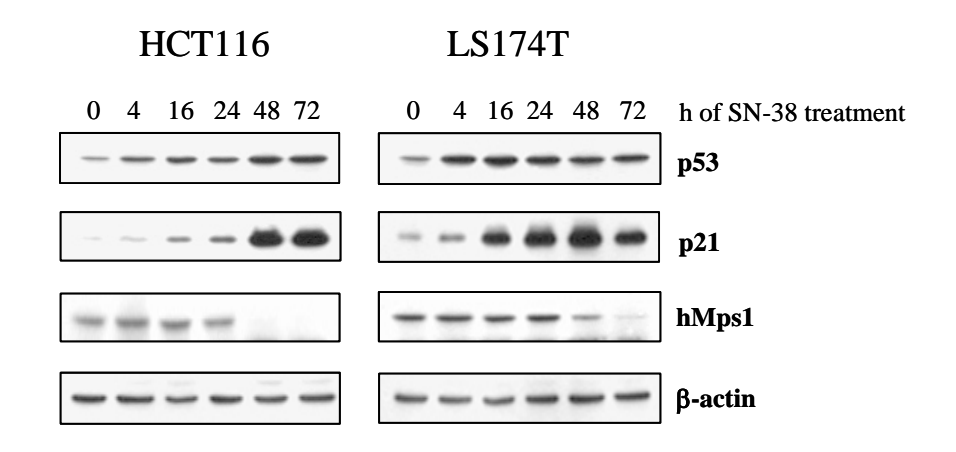
Comparison of p53 and p21 expression achieved after SN-38 treatment and after adenoviral transduction

HCT116 cells were treated with SN-38 for 2 days or were transduced with various MOI of Adp53<sup>wt</sup> and the expression of p53 and p21 were compared. The figure shows that an MOI of 20 is necessary to achieve a level of p21 comparable to that induced after SN-38 treatment.



#### **Supplementary figure S4B**

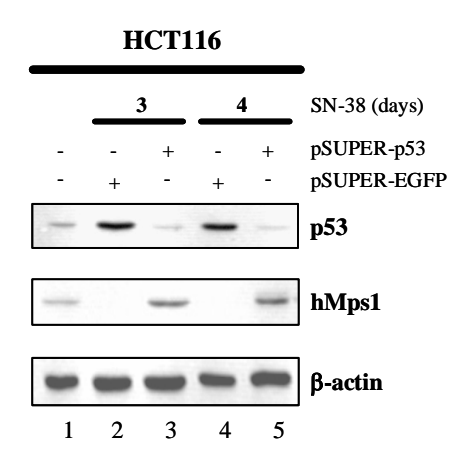
Time course of hMps1 suppression in p53<sup>wt</sup> cell lines during SN-38 treatment (10 nM). hMps1 suppression in HCT116 and LS174T cell lines begins at 48 h after treatment, only after both p53 and p21 are highly upregulated.



# **Supplementary figure S5**

Suppression of p53 leads to upregulation of hMps1 in SN-38-treated HCT116 cells.

HCT116 cells were transfected with pSUPER-EGFP or pSUPER-p53 and the expression of hMps1 was analysed by Western blotting. The figure shows that SN-38 treatment leads to downregulation of hMps1 (lanes 2 and 4) and that the suppression of p53 leads to the reexpression of hMps1 (lanes 3 and 5).



# DNA Damage-induced Expression of p53 Suppresses Mitotic Checkpoint Kinase hMps1: THE LACK OF THIS SUPPRESSION IN p53MUT CELLS CONTRIBUTES TO APOPTOSIS

Mandar R. Bhonde, Marie-Luise Hanski, Jan Budczies, Minh Cao, Bernd Gillissen, Dhatchana Moorthy, Federico Simonetta, Hans Scherübl, Matthias Truss, Christian Hagemeier, Hans-Werner Mewes, Peter T. Daniel, Martin Zeitz and Christoph Hanski

J. Biol. Chem. 2006, 281:8675-8685.

doi: 10.1074/jbc.M511333200 originally published online January 30, 2006

Access the most updated version of this article at doi: 10.1074/jbc.M511333200

#### Alerts:

- When this article is cited
- · When a correction for this article is posted

Click here to choose from all of JBC's e-mail alerts

#### Supplemental material:

http://www.jbc.org/content/suppl/2006/02/07/M511333200.DC1.html

This article cites 50 references, 25 of which can be accessed free at http://www.jbc.org/content/281/13/8675.full.html#ref-list-1